

Recent Results from RMP ELM suppression experiments in DIII-D

R.A. Moyer, J.A. Boedo, V.A. Izzo, I. Joseph,
S. Mordijck, D.L. Rudakov, J.H. Yu, *UCSD*

T.E. Evans, N.H. Brooks, T.H. Osborne, P. Gohil,
J.S. deGrassie, A.W. Leonard, T.W. Petrie *GA*

M.E. Fenstermacher, M. Groth, C.J. Lasnier, *LLNL*

J.G. Watkins, *SNL*

T.C. Jernigan, *ORNL*

M. Jakubowski, O. Schmitz, *FZJ*

T.L. Rhodes, L. Schmitz, G. Wang, A.E. White, L. Zeng,
E.J. Doyle *UCLA*

G.R. McKee *U. Wisc.*

C. Rost, J.R. Dorris *MIT*

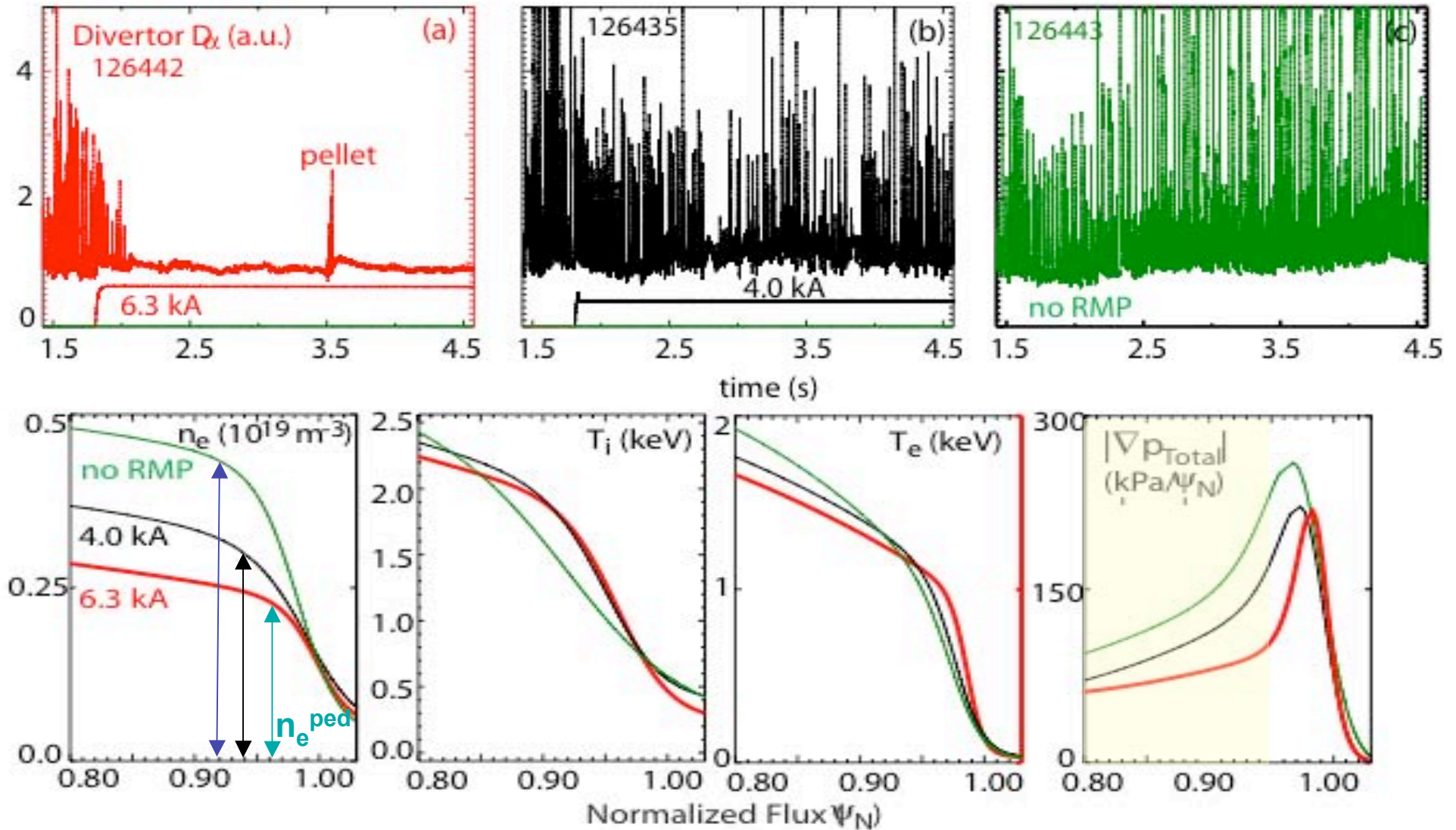
3rd Error/Non-Axisymmetric Magnetic Field Workshop
Orlando, Florida

November 16, 2007

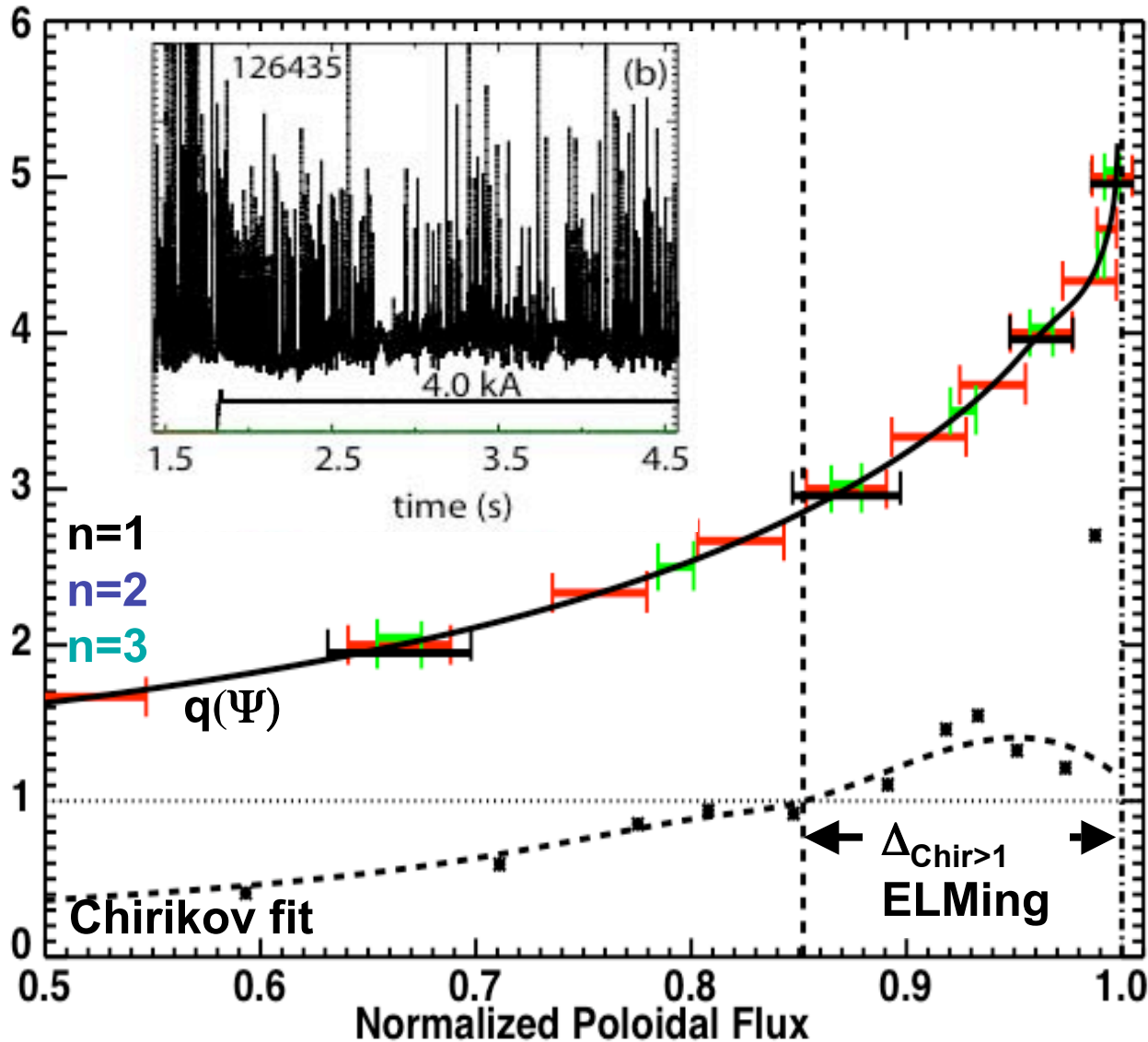
Recent results from RMP ELM suppression experiments highlight critical uncertainties

- **Plasma response to the RMP** is being investigated with 3 magnetic field models :
 - **TRIP3D vacuum field model** (no plasma response):
 - Predicts strike point footprints in the particle flux (but not heat flux) [O. Schmitz and M. Jakobowski, FZJ; Watkins, SNL; **Joseph, UCSD this workshop**]
 - Operationally predicts ELM suppression based on width of vacuum field magnetic island overlap region [Fenstermacher, et al.]
 - **IPEC Ideal Perturbed Equilibrium Code**: Park, Menard, and Boozer: **[Park, Boozer this workshop]**
 - Application to RMP ELM control cases beginning
 - 2-state magnetic field model:
 - outer % in Ψ_N with full vacuum field/stochastic \rightarrow reproduce footprints
 - Ideal perturbed equilibrium inside of the stochastic region; where is the boundary between the perturbed equilibrium and the stochastic layer?
 - **Extended MHD**: JOREK [Nardon and Becoulet], NIMROD [Izzo, Kruger], M3D [Strauss]
 - Predict formation of $E \times B$ convection cells that enhance particle transport
 - Rotation leads to “screening” of the applied RMP, but not yet using rotation profile in experiments (counter-toroidal rotation just inside separatrix)
 - RMP rise time $\tau_{RMP} \rightarrow 0$ in toroidal simulations (Izzo); impact of finite $\tau_{RMP} \sim 20$ ms τ_{rec} being investigated in reduced (slab) geometry [Kruger]

Plasma profile changes suggest that RMP effect in the region $0.8 < \Psi_N < 0.95$ might be important

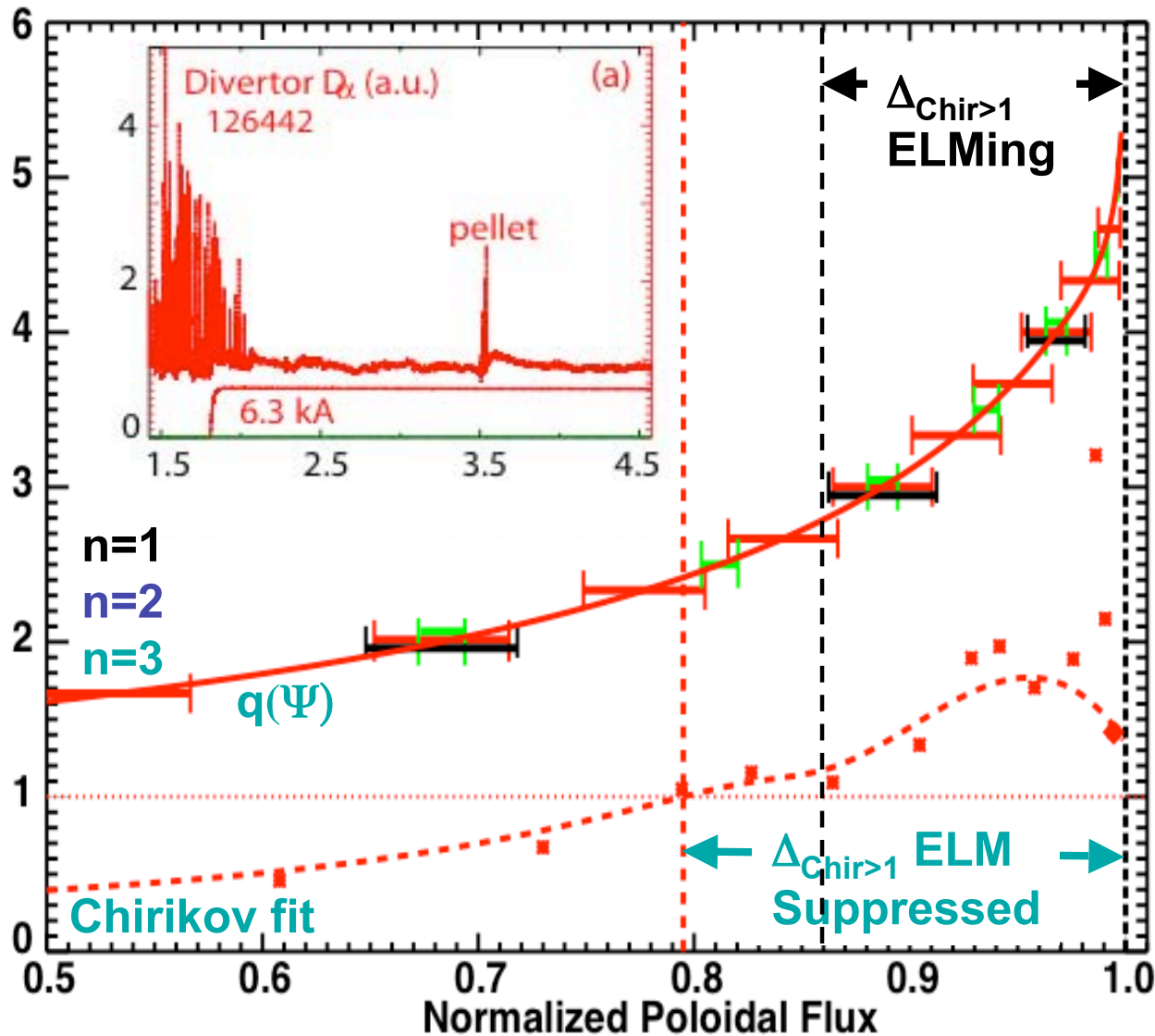


At Low I-coil Current Islands in Vacuum Field Model Overlap Beyond Pedestal But ELMs Remain



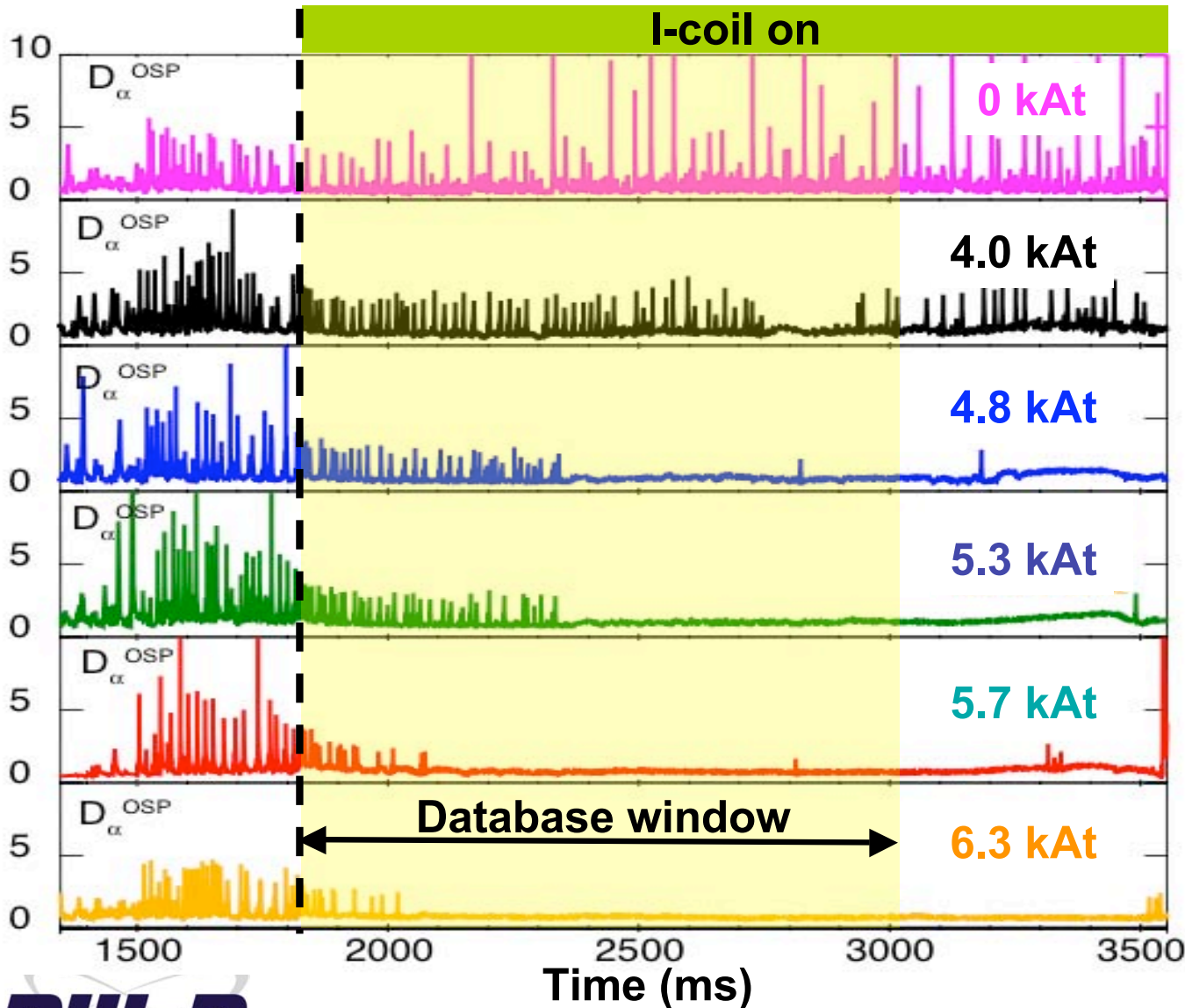
- Chirikov parameter $\sigma_{\text{CH}} = \frac{\text{(average island size)}}{\text{(island separation)}}$
- Strong stochasticity for $\sigma_{\text{CH}} > 1.0$
- Vacuum island overlap (SURFMN) satisfies Chirikov parameter > 1.0 from edge to $\Psi_N = 0.85$
 - $\Delta_{\text{Chir}>1} = 0.15$
- Note $\Delta_{\text{Chir}>1} / \Delta_{\text{ped}} \sim 2.8$

During ELM Suppression Magnetic Island Overlap Region in Vacuum Field Model Larger



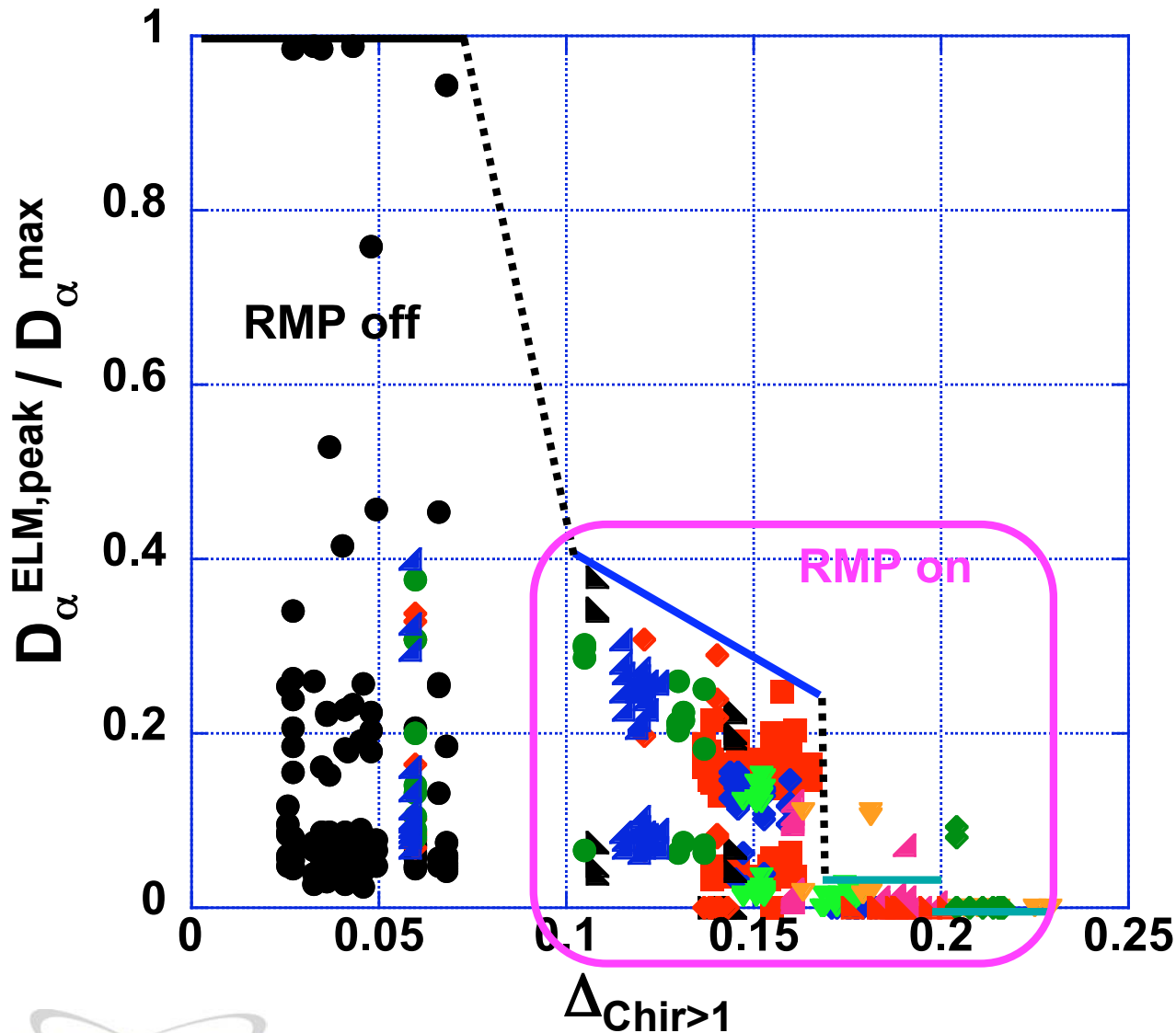
- Vacuum island overlap satisfies $\sigma_{\text{CH}} > 1.0$ from edge to $\Psi_N = 0.8$
 - Island overlap width $\Delta_{\text{Chir}>1} = 0.20$
- Note $\Delta_{\text{Chir}>1} / \Delta_{\text{ped}} \sim 4.3$
- Suggests correlation of threshold $\Delta_{\text{Chir}>1}$ and ELM suppression
 - Possible range $0.15 < \Delta_{\text{Chir}>1} < 0.20$

I-coil Current Scan at Fixed Shape and q_{95} Produces Systematic Change in ELM Behavior



- Provides multi-ELM sampling
 - 24 kinetic EFIT timeslice windows per shot
 - Multiple ELMs for many of the EFIT windows
- Similar sampling of other scans
- Complete suppression earlier at higher I-coil current

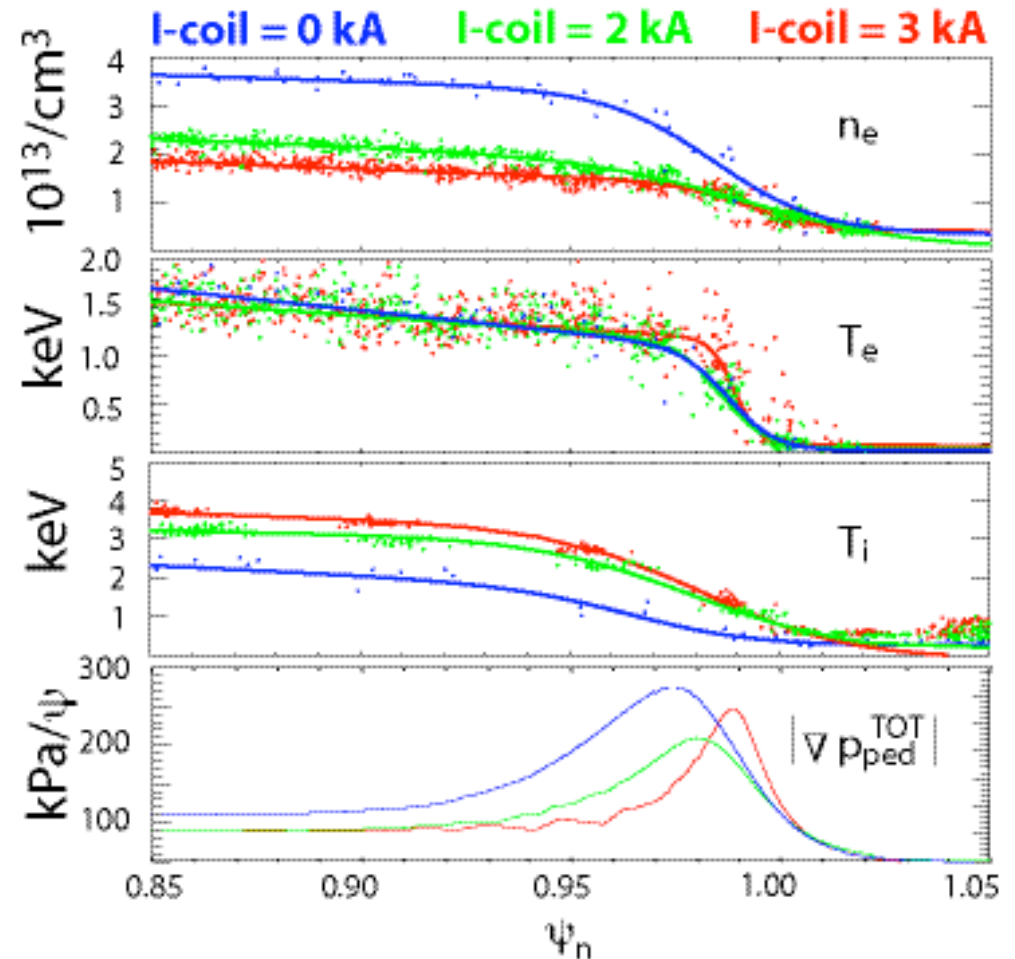
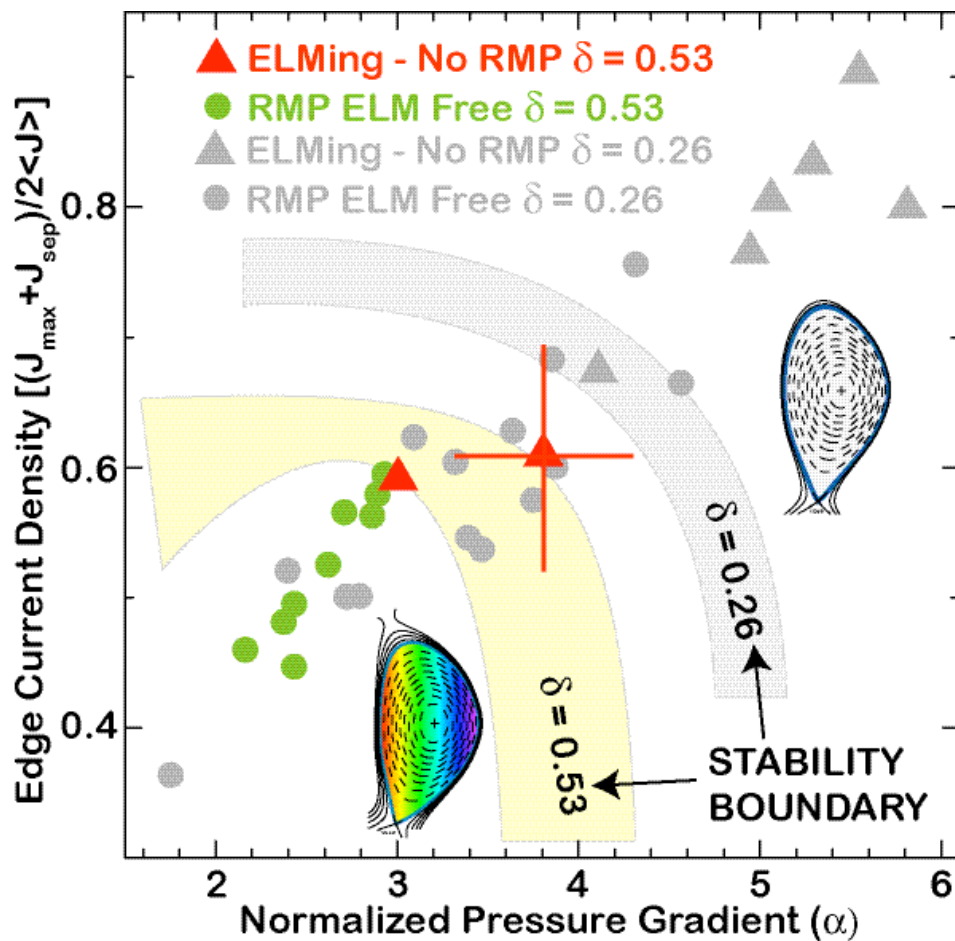
Maximum ELM Size Correlated with Width of Edge Region Satisfying $\sigma_{CH} > 1.0$



- ELM size from fast D_{α} at outer divertor strikepoint
 - Normalized to largest ELMs without RMP in database
- Full spectrum of ELM sizes both without and with RMP
 - Consistent with non-linearity of ELM instability

RMP ELM-suppressed H-modes are linearly stable to peeling-ballooning modes.

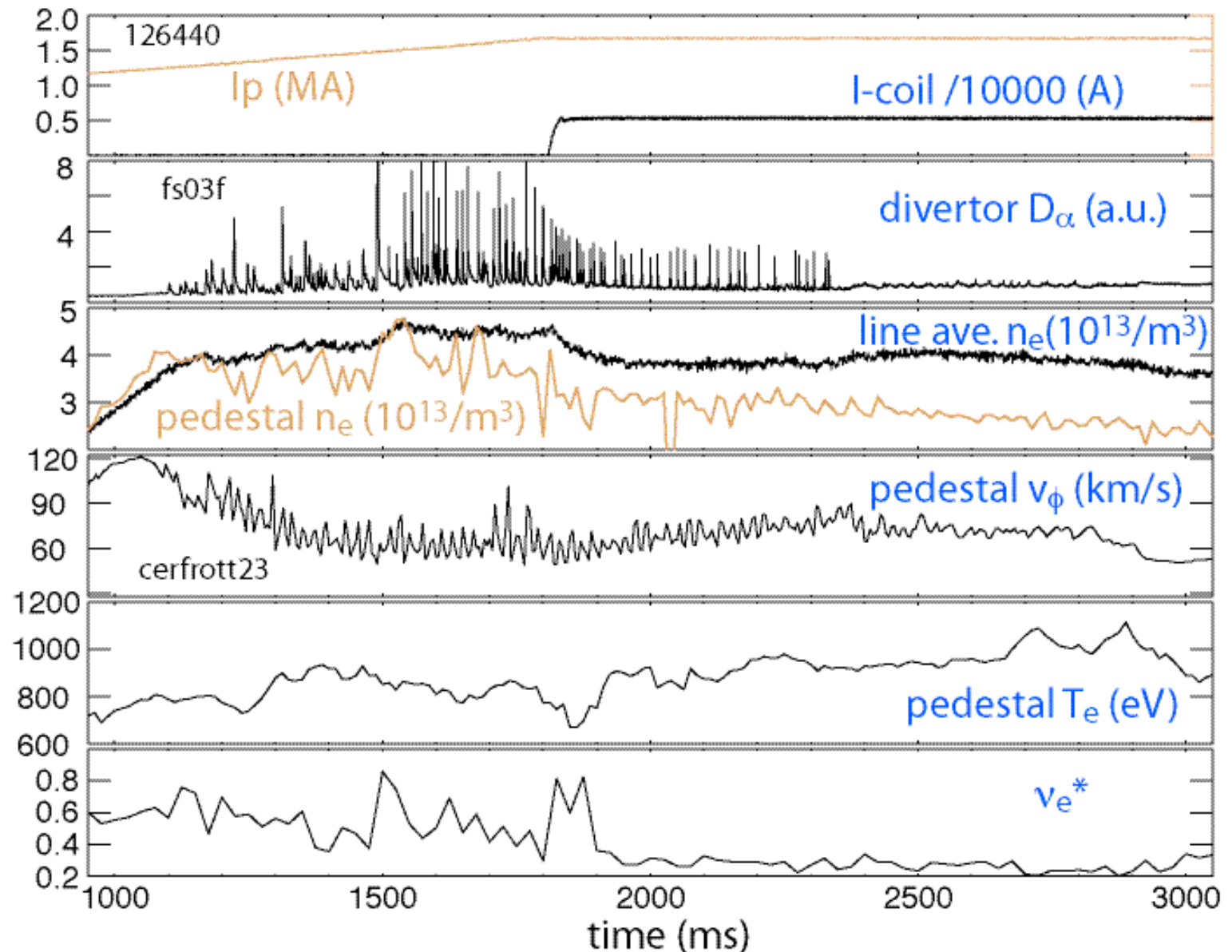
- Largest change in pedestal density profile \rightarrow critical to understand global particle balance and particle transport.



Density pumpout is not sufficient to stabilize ELMs

- ELMs remain after **pumpout** is over until resonant window for **suppression** and vacuum island overlap
- Indicates a missing parameter controlling ELM suppression

Fenstermacher
BI1.00002

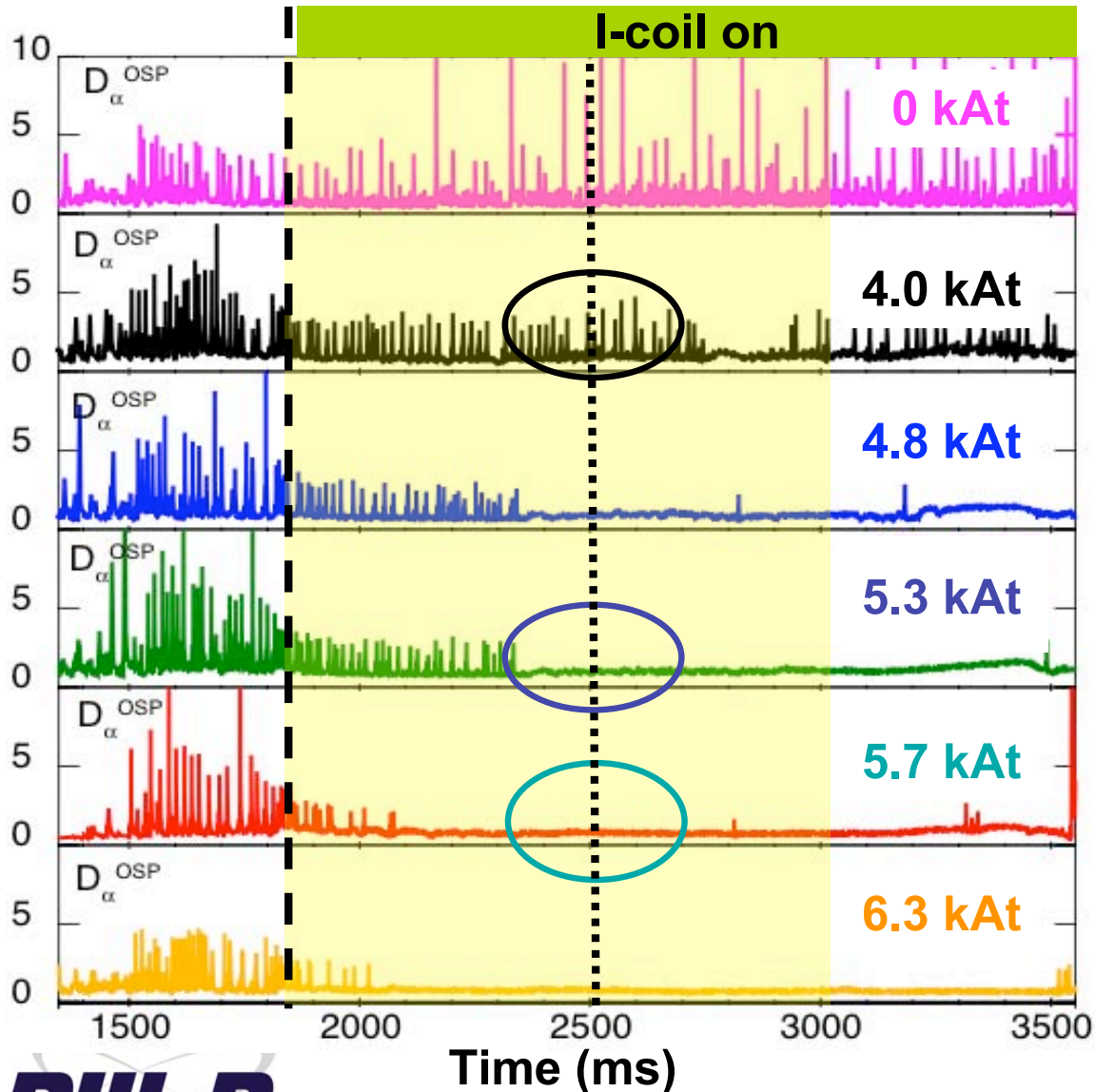


Transport model should provide increased particle but only weak ($\sim 2x$) increase in electron thermal transport

Stochastic layer transport:

- Electron thermal transport in vacuum field model destroys H-mode pedestal [**Joseph PSI 07; SFP 07 submitted to Nucl. Fusion 07**]
- Need to “shut off” parallel electron heat conduction...
 - Sheaths and Flux-limited transport at low collisionality [**Tokar PRL 07**]
 - Electrostatic confinement of electrons in $\phi_{pl} \sim T_e$ potentials [**XGC: Park, Chang**]
 - ϕ at target plates \rightarrow -100s of V with footprint structure in RMP ELM suppressed discharges [**Watkins, SNL**]; E_r in boundary integrates to $\sim T_e$ at $\Psi_N = 0.99$ (500 eV)
- ...while enhancing cross-field particle transport:
 - Increased SOL convective transport (“blobs”) during RMP ELM suppression [**Boedo EPS07, APS07**]
 - $E \times B$ convection cells in remnant island region
 - Potentials modified by islands and sheaths of lost field lines; measured in TEXT Ergodic Magnetic Limiter experiments [**Takamura PF (87), Evans EPS (87), Wooton JNM (90)**]
 - Predicted in extended MHD modeling (**JOREK: Nardon and Becoulet; NIMROD: Izzo**)
 - Increased drift wave turbulence due to E_r modifications [**Moyer IAEA06, APS07**]
 - E_r changes measured for $0.7 < \Psi_N < 1$ when RMP is applied (before ELM suppression)
 - increase in broadband \tilde{n}_{rms} for $0.75 < \rho < 1$ at both ion ($k_\theta \sim 1$ inv. cm) and electron ($k_\theta \sim 4-5$ inv. cm) scales
 - \tilde{n}_{rms} increases $2x \rightarrow \Gamma \rightarrow \tilde{n}_{rms}^2 \rightarrow 4x$ consistent with density change

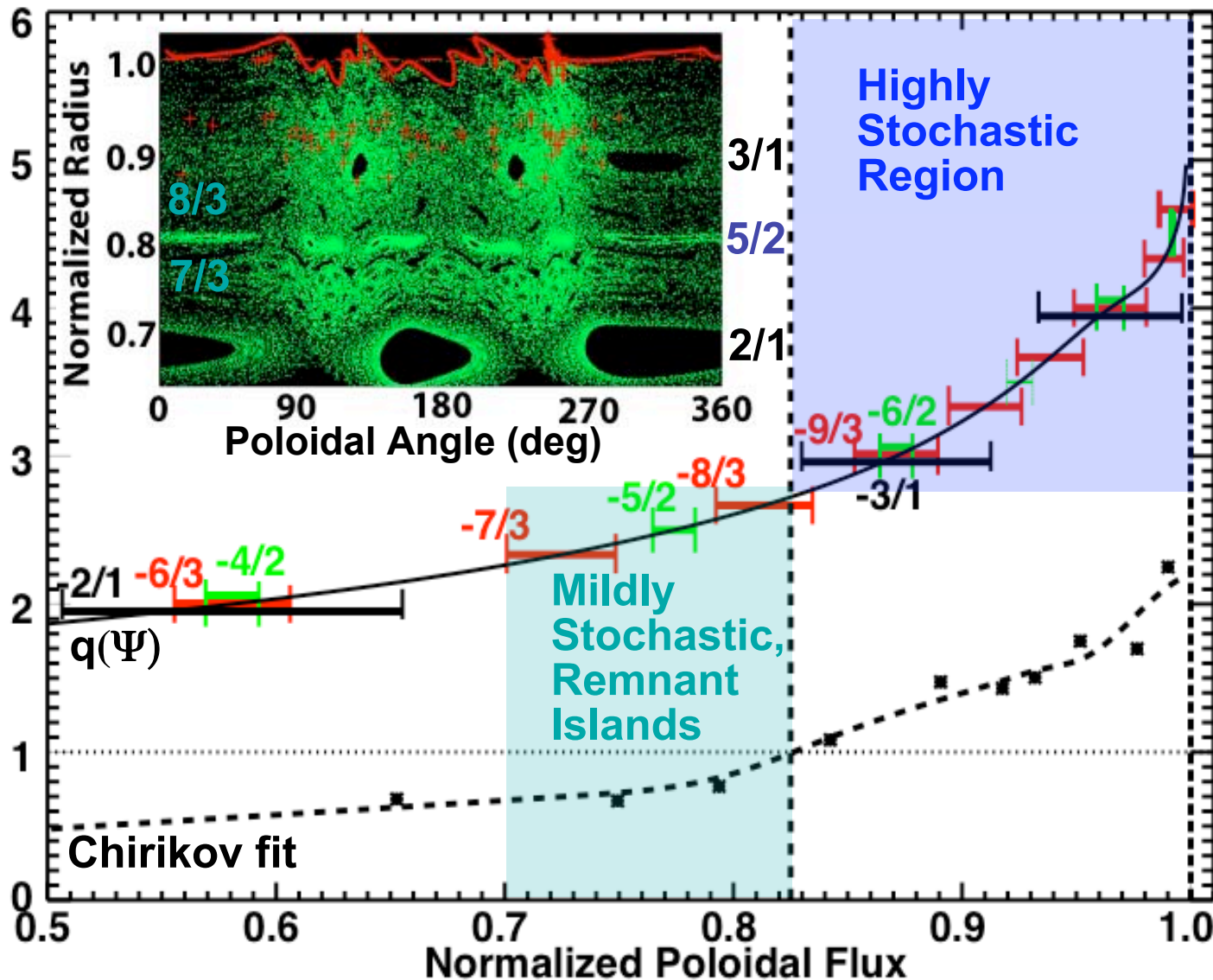
Is ELM Size Ordering by $\Delta_{\text{Chir}} > 1$ Due to Field Line Loss from Remnant Island Region?



- Multiple suggestions [1-3] that ExB convective cells could play a role if threshold region contains:
 - Remnant islands
 - Field lines with short connection length to targets
- Field line tracing (TRIP3D) in kinetic EFIT + RMP vacuum fields
 - Compare ELMing vs ELM suppressed cases

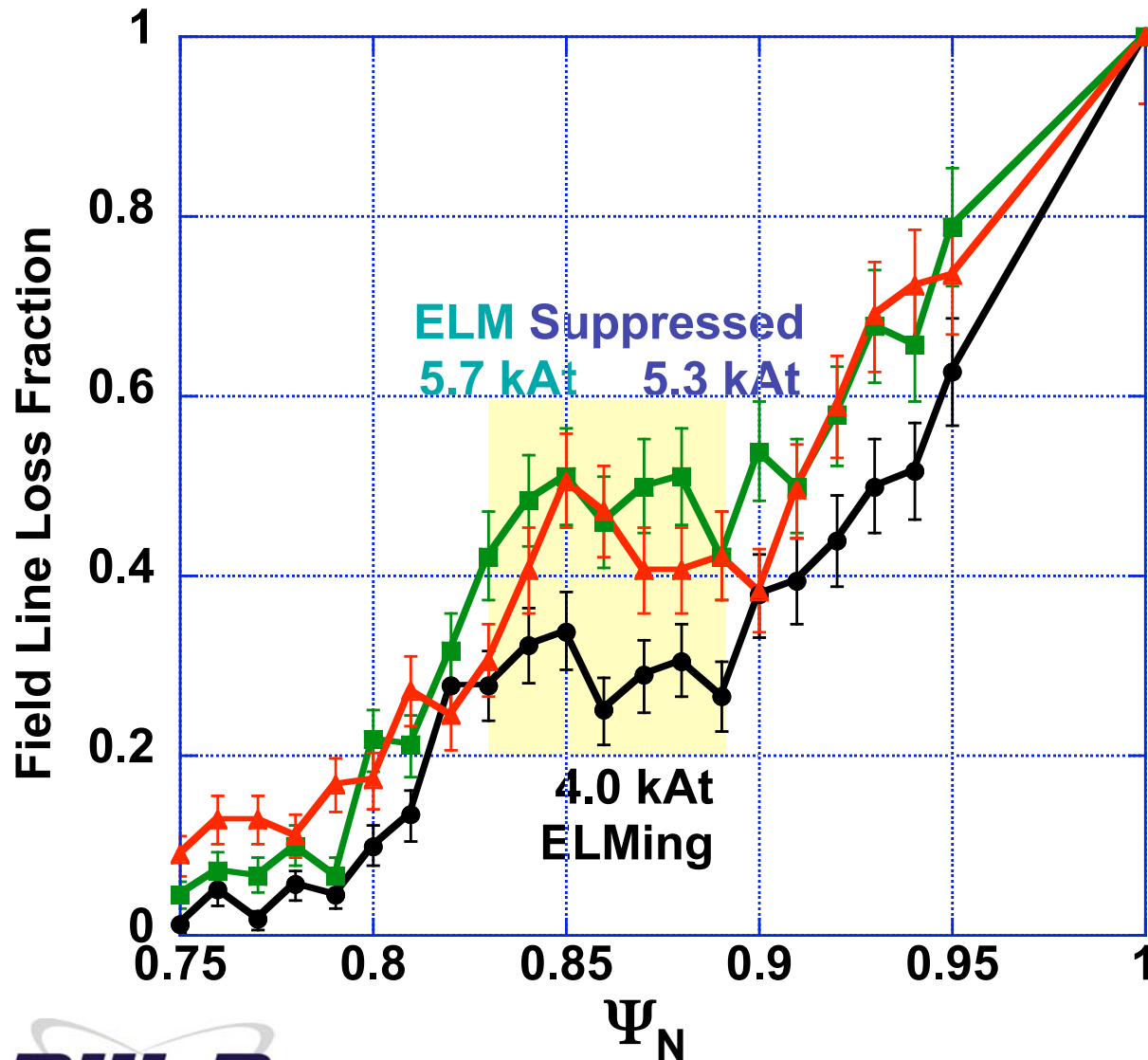
1. Takamura PF (1987)
2. Evans EPS (1987)
3. Wooton JNM (1990)

Vacuum Field Contains Remnant Islands Adjacent to Stochastic Region



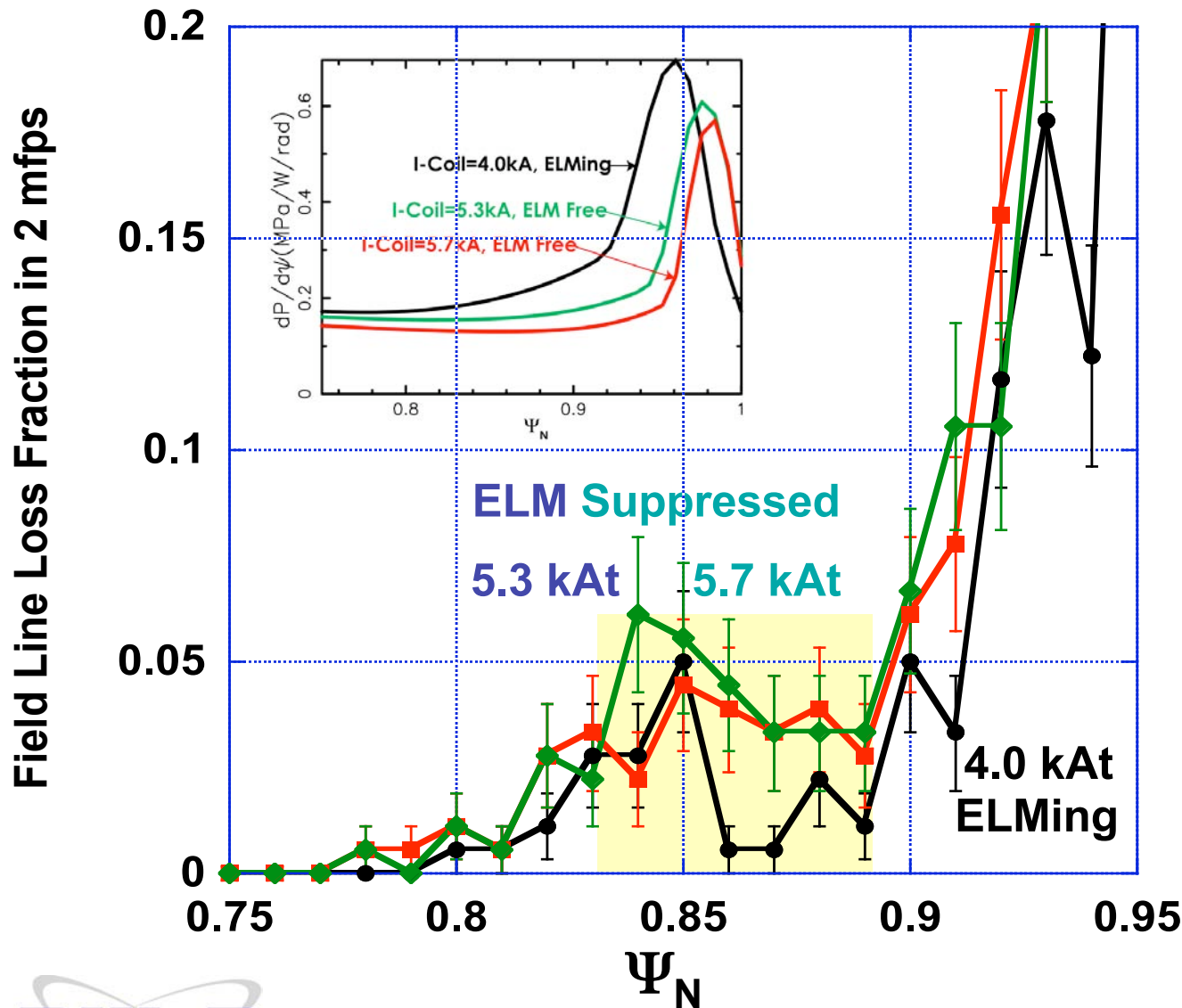
- Stochastic region from $q \sim 3$ surface outward
- Remnant islands at $q = 8/3, 5/2, 7/3$ surfaces may be weakly coupled

Field Line Loss Fraction From Remnant Island Region $0.83 < \Psi_N < 0.89$ Higher in ELM Suppressed Cases



- Traced field lines
 - Launched with uniform poloidal distribution on unperturbed flux surfaces
 - Forward traced until strike outer divertor or 200 toroidal transits
- Field line loss fraction up to 2x higher for $0.83 < \Psi_N < 0.89$

Field Line Loss Fraction with Short Connection Length Higher in ELM Suppressed Cases

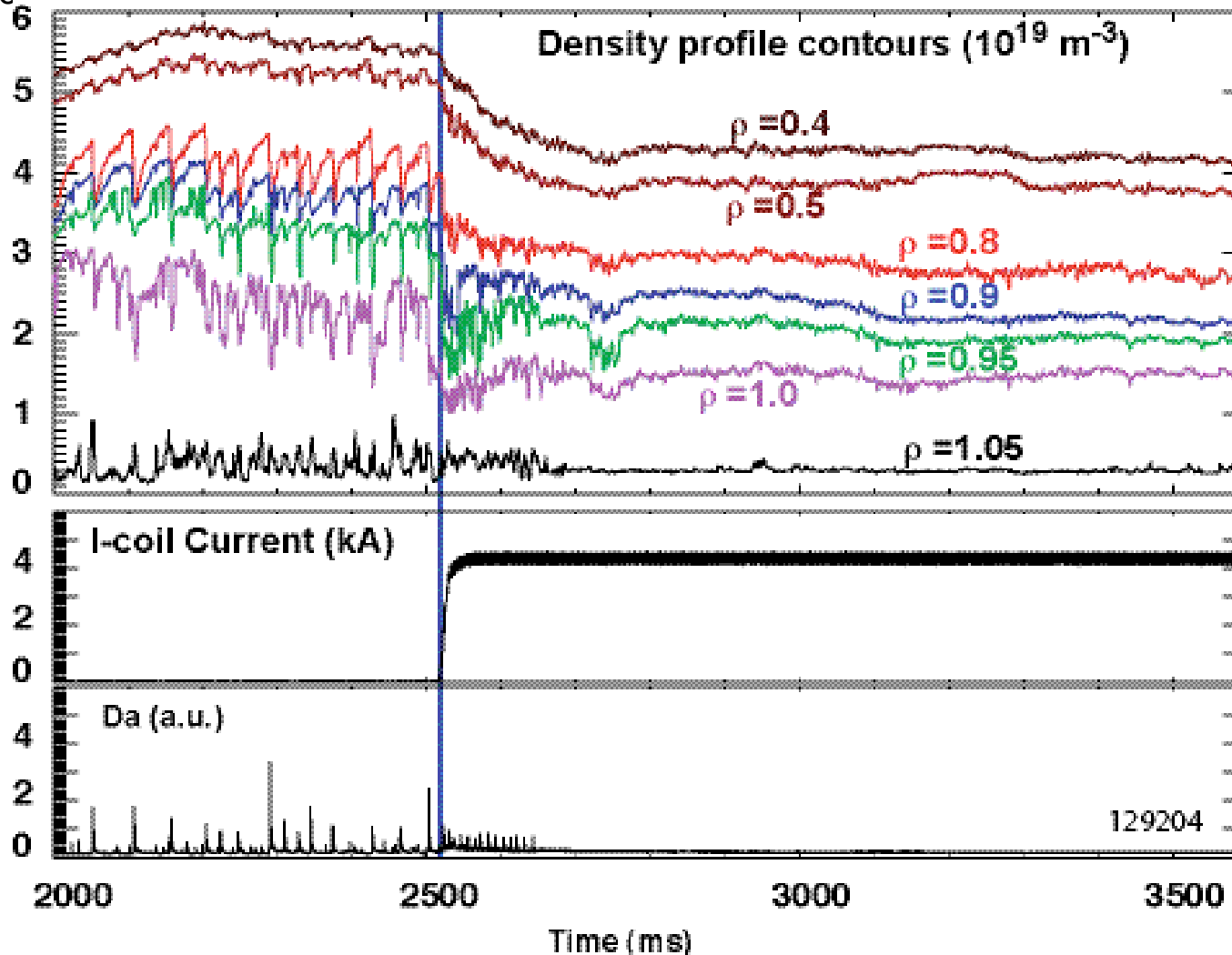


- Criterion for “short” connection length: $L_c < 2 * \lambda_{ei}$ (electron-ion collisional mean free path in pedestal)
- Short connection length to divertor targets affects potential deep in edge plasma
 - ExB convection cells may play a role in changes to plasma profiles

Boedo Oral GO3.02 Tu pm
Moyer, Watkins, Zeng
Poster session UP8 Th pm

Density profile evolution has a 2-step character: fast pedestal change and longer core change

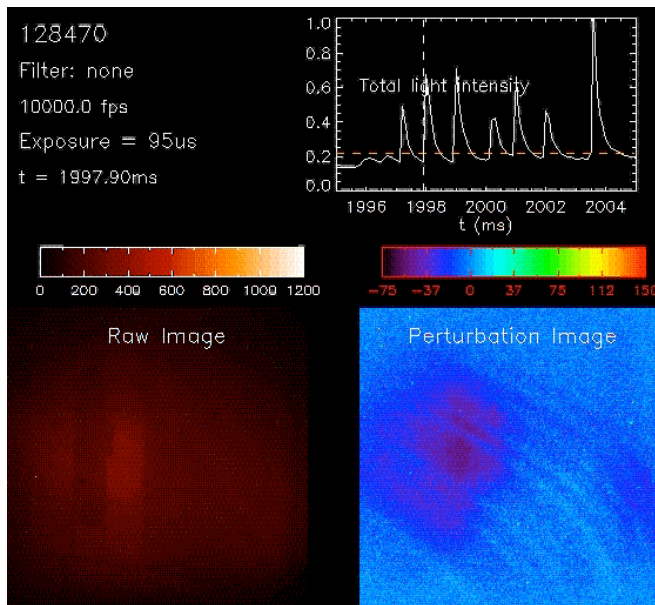
- Pedestal n_e drops with e-folding time of 77 ms [Zeng UP8.00026], followed by a broadening at the base [Boedo, G03.00002]
- Core n_e drops with e-folding time of 815 ms \rightarrow adjustment to new b.c.?



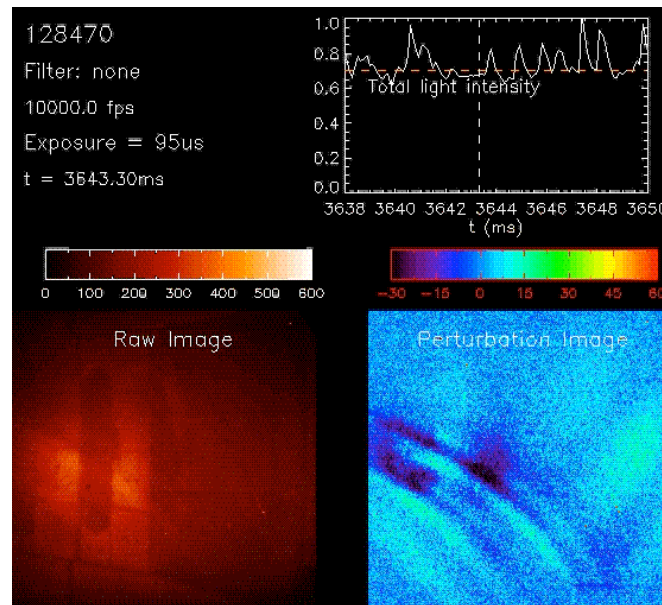
Filamentary structures in ELMing H-mode persist during RMP pulse (both ELMing and suppressed)

- visible emission from tangentially viewing UCSD fast framing camera **J. Yu UP8.00030**

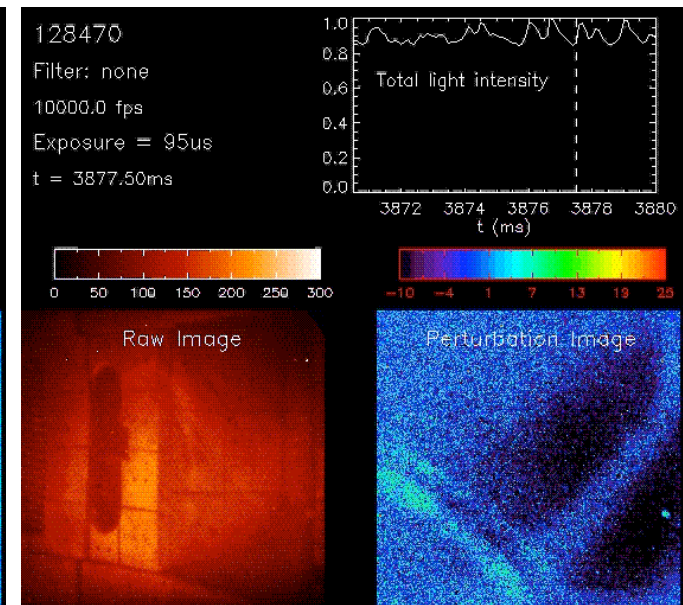
I-coil off inter-ELM



I-coil on inter-ELM

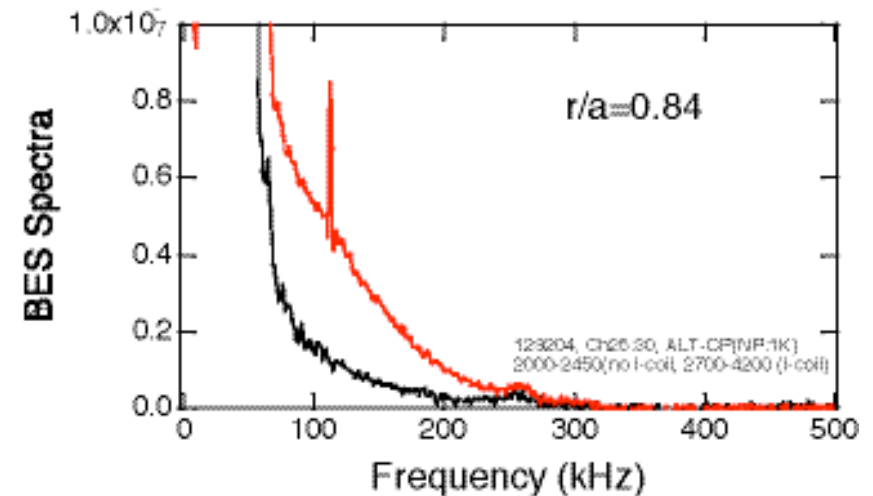
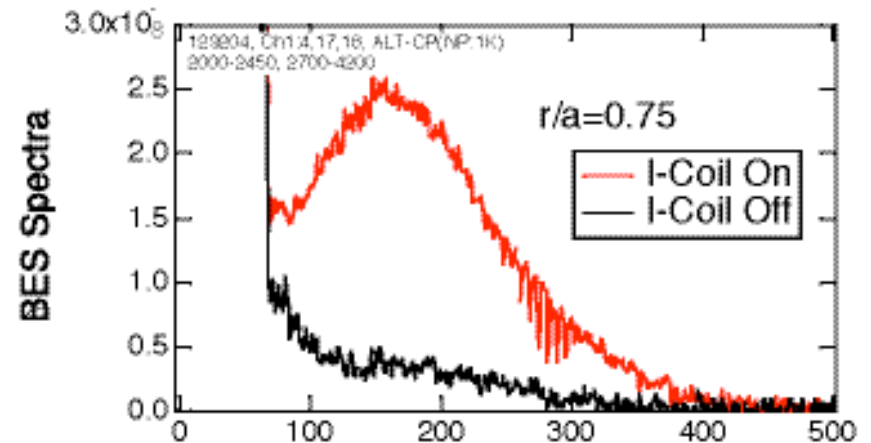
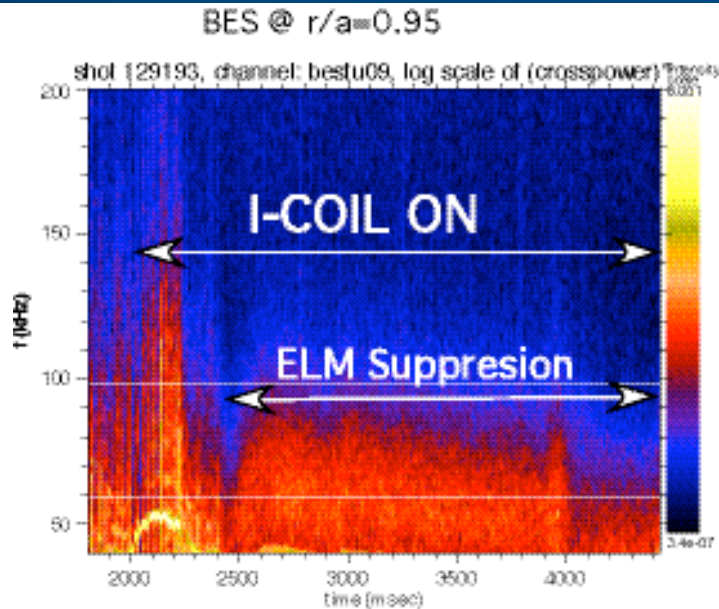


I-coil on ELM suppr

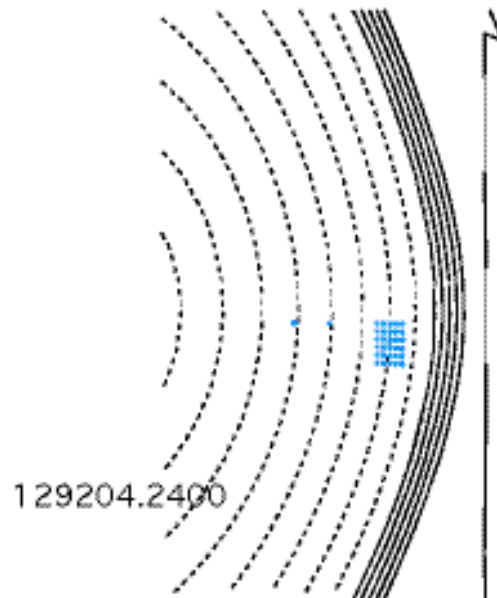


- Increased intermittent transport in boundary during RMP → large particle but little thermal transport **Boedo G03.00002**

Ion scale fluctuations increase broadband across a wide radial extent $0.75 < \rho < 1$ when ELMs suppress

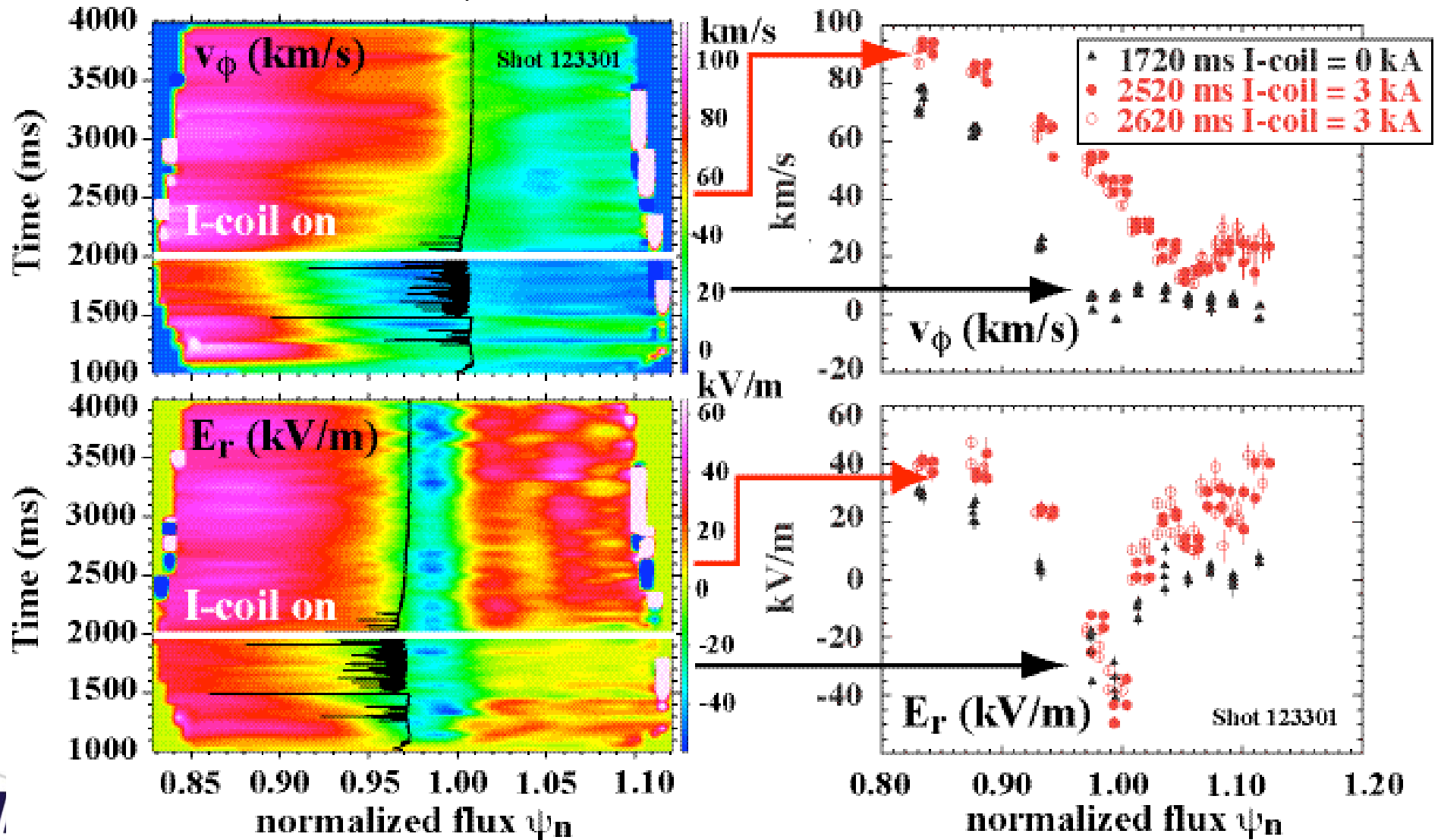


BES analysis
by G.R.
McKee, Un
of Wisc.-
Madison



Pedestal toroidal rotation and E_r change promptly when RMP is applied and edge q resonant ($3.4 < q_{95} < 3.7$).

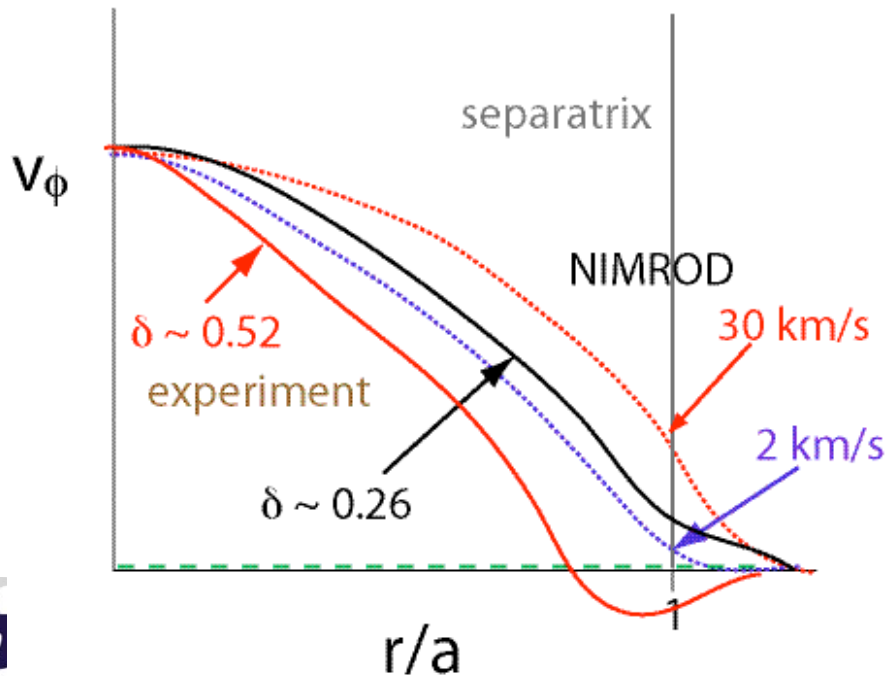
- H-mode pedestal v_ϕ spins up and E_r well narrows.



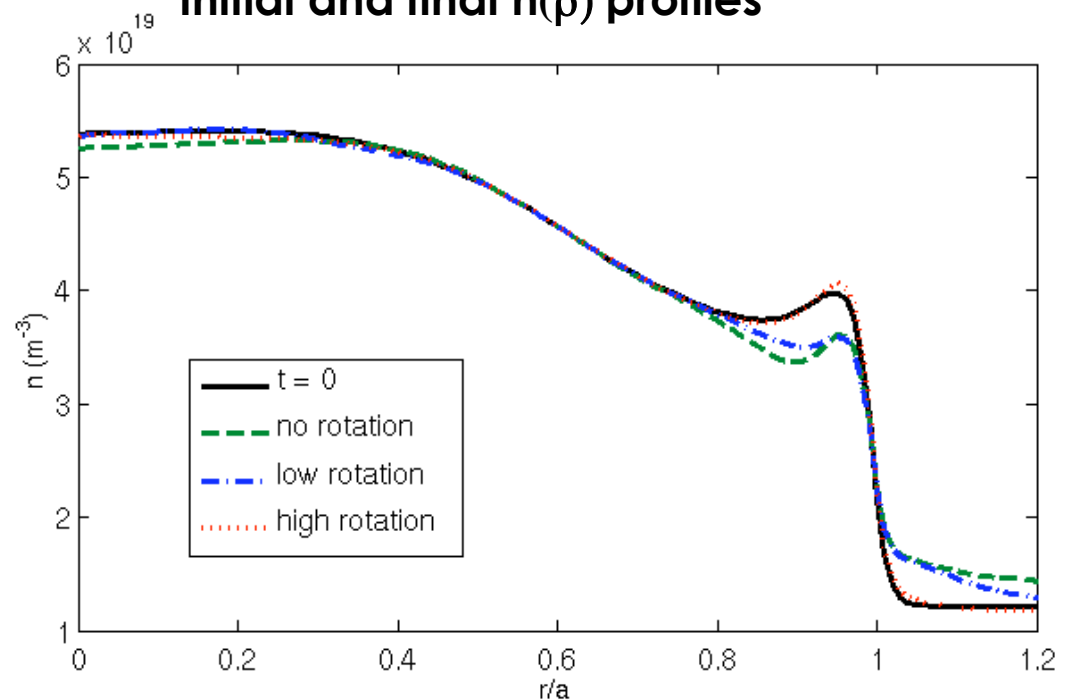
Extended MHD runs with JOREK and NIMROD predict formation of $E \times B$ convective cells

- JOREK simulations by E. Nardon & M. Becoulet
- Numerical experiments with NIMROD extended MHD code in full toroidal geometry [V. Izzo](#)
 - Uses ELM milestone equilibrium developed by D. Brennan and much higher resistivity
 - Experiments are near the no-wall limit $\beta_n \sim 2.4 I_i \rightarrow$ equilibrium unstable
 - instant rise time τ_{RMP} : experiment $\tau_{RMP} = 20$ ms: $\tau_A \ll \tau_{rec} \sim \tau_{RMP} \ll \tau_R$
 - Effect of τ_{RMP} on plasma response & RMP penetration studied with NIMROD in reduced (slab) geometry: [Kruger Poster UP8.00025](#)

Qualitative Representation of Rotation Profiles



Initial and final $n(\rho)$ profiles

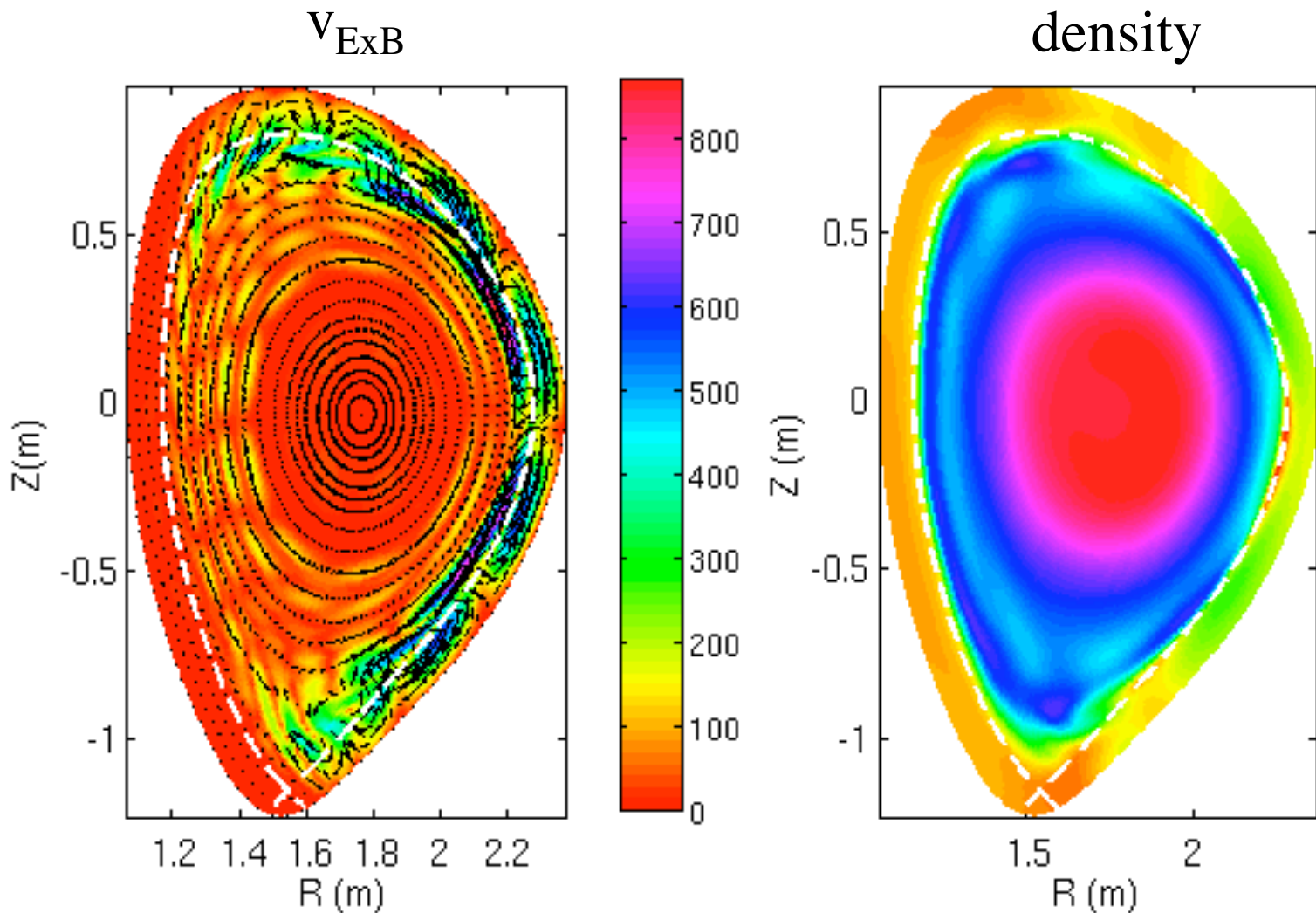


$E \times B$ convection cells form across separatrix for $v_\phi = 0$ and increase radial particle transport into $\rho \sim 0.7$

- Contours of v_{ExB} (km/s) and density show particle transport modification in to $\rho \sim 0.7$ without toroidal rotation (vacuum field perturbation).

$V_\phi = 0$
case

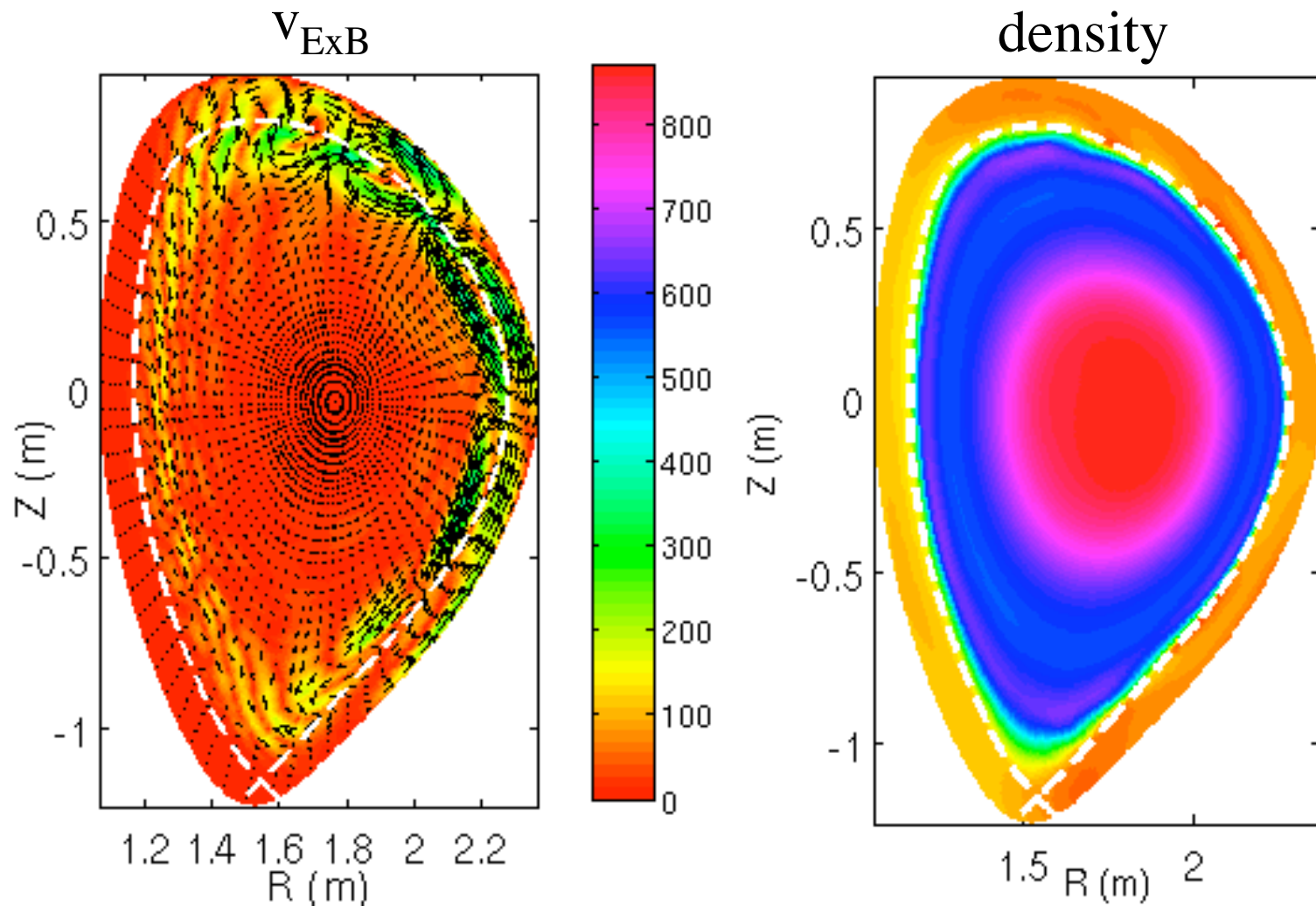
NIMROD
results
provided
by
V. Izzo



In high v_ϕ case, $E \times B$ convection cells exist, but at lower amplitude with little effect on density profile

- Contours of $v_{E \times B}$ (km/s) and density show transport modification localized to separatrix with high v_ϕ (significant screening of RMP).

High
 v_ϕ
case



Summary and Conclusions

- Fusion community appears polarized on the RMP ELM suppression results:
 - (largely tokamak) school of thought: parallel electron heat conduction is robust even with the limitations of Rechester-Rosenbluth so the pedestal T_e has to drop (that is, χ_e must increase more than a factor 2) if the outer 15%+ of the plasma is stochastic (1/3 of the plasma volume!)
 - (other, including RFP & helical device) school of thought: the ratio of particle transport to thermal conduction in stochastic fields is “anomalous” **[I.e. Ding this morning]**;
- Physics missing from RR transport may “shut off” parallel electron heat conduction:
 - Flux limits to parallel heat conduction at low collisionality **[Tokar]**
 - Electrostatic confinement of electrons in the open flux tubes (yes, the boundary might look like a mirror!)
 - ✓ Appears consistent qualitatively with experimental results
 - ✓ seen in XGC numerical experiments using resonant field amplification of vacuum field **[Park this APS]**
 - ✓ GAMMA-10 uses ECH to spin the plasma after plugging, producing multi-keV electron and ion temperatures **[this APS]**
 - ✓ Maryland Mirror experiment applies the rotation with a center rod/electrode
 - Sheared rotation: The “ion root” in stellarators - breaking axisymmetry induces a radial current, $\mathbf{j} \times \mathbf{B}$ force, and **sheared rotation**
 - ✓ ambipolar potential has enough E_r shear to suppress transport

Summary and Conclusions - II

- Whatever the result for parallel thermal conduction...
 - RMP is screened and no open field lines versus
 - some form of “plugging” of electron parallel losses on open field lines)
- ...we need some form of enhanced particle transport (convection) to account for the density profile changes:
 - convective “blob” transport increases in experiment (is it enough?)
 - $E \times B$ convective cells measured in previous EML experiments
 - $E \times B$ convective cells seen in extended MHD models of plasma response in toroidal geometry
 - scaling with dissipation/viscosity, which is 100x the experiment
 - effect of RMP rise time on final state (“error field” or “forced reconnection”?)
 - $\mathbf{j} \times \mathbf{B}$ should efficiently damp the (axisymmetric) Zonal flow that regulates turbulence: consistent qualitatively with exp.
- Many groups are working on these issues (Thank you!) - but ITER needs answers urgently and we can always use more help!

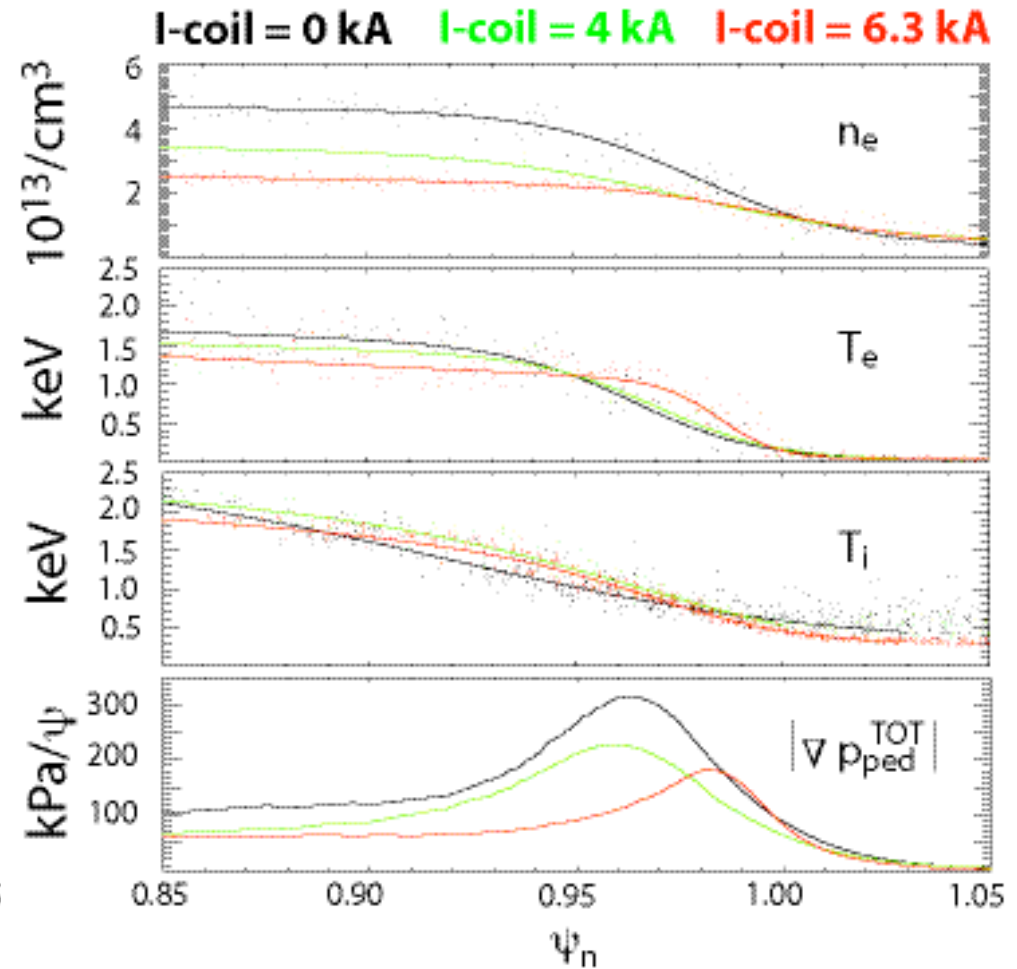
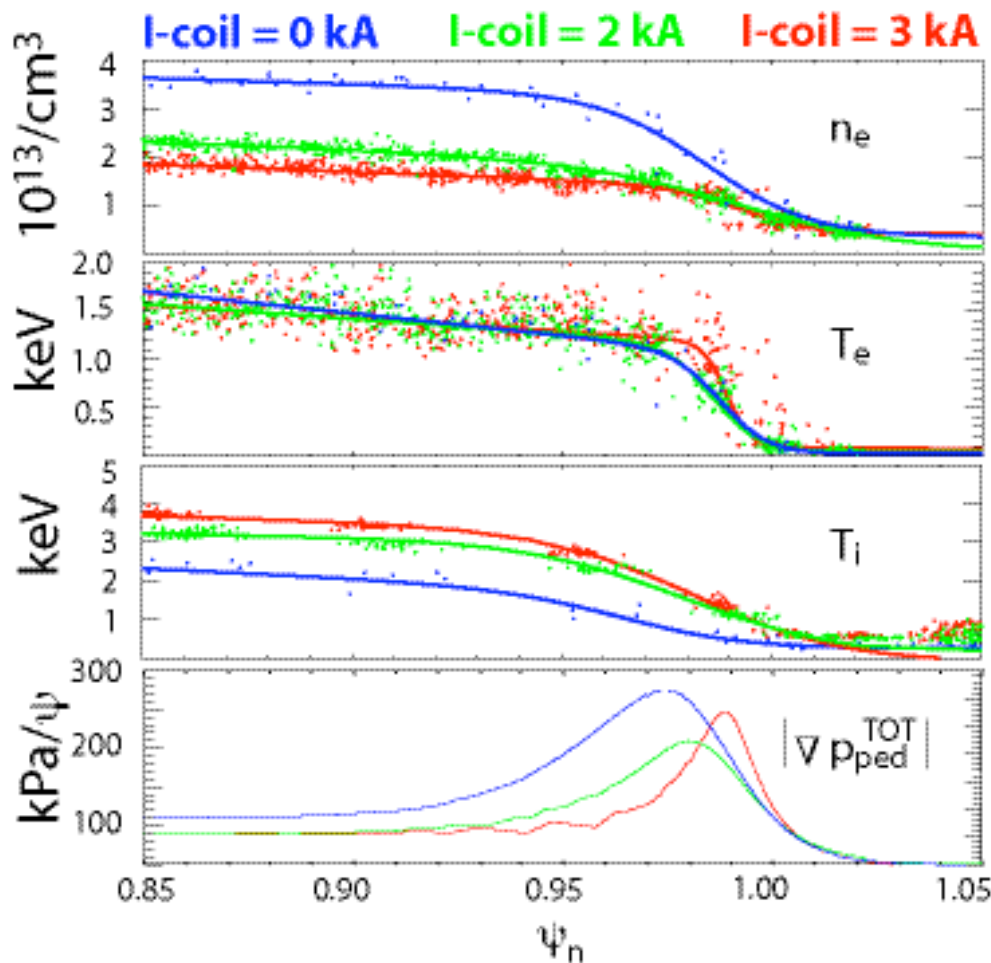
Backup slides

I-coil RMP has largest effect on density profile, not T_e profile at low collisionality.

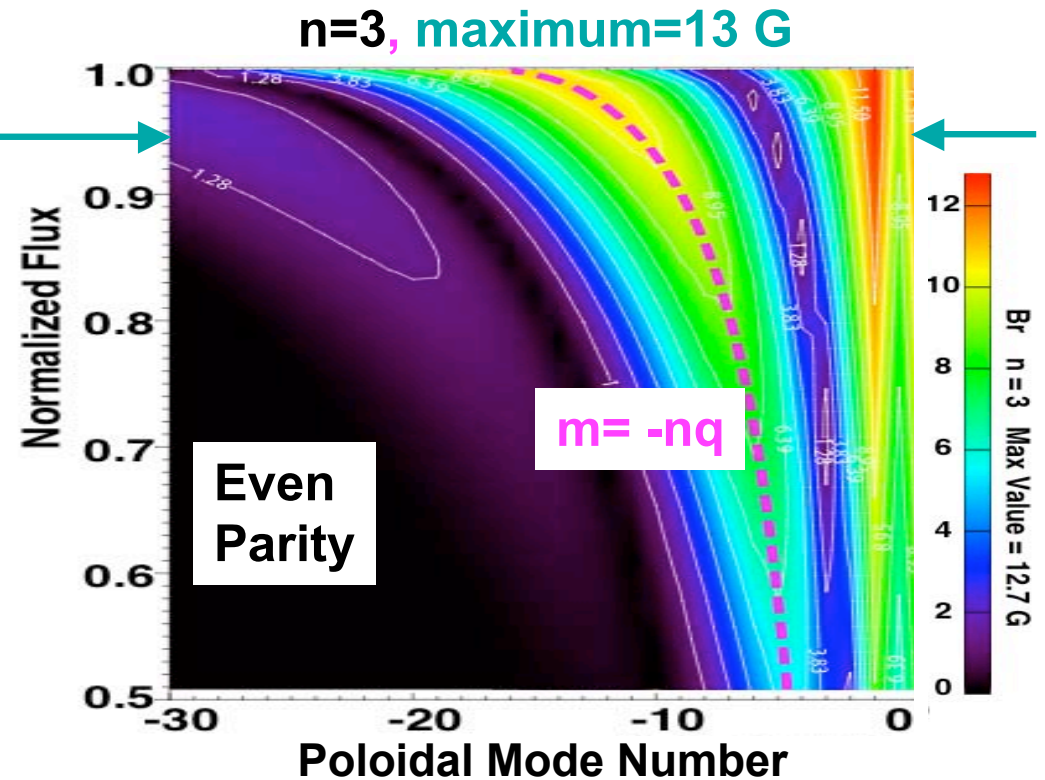
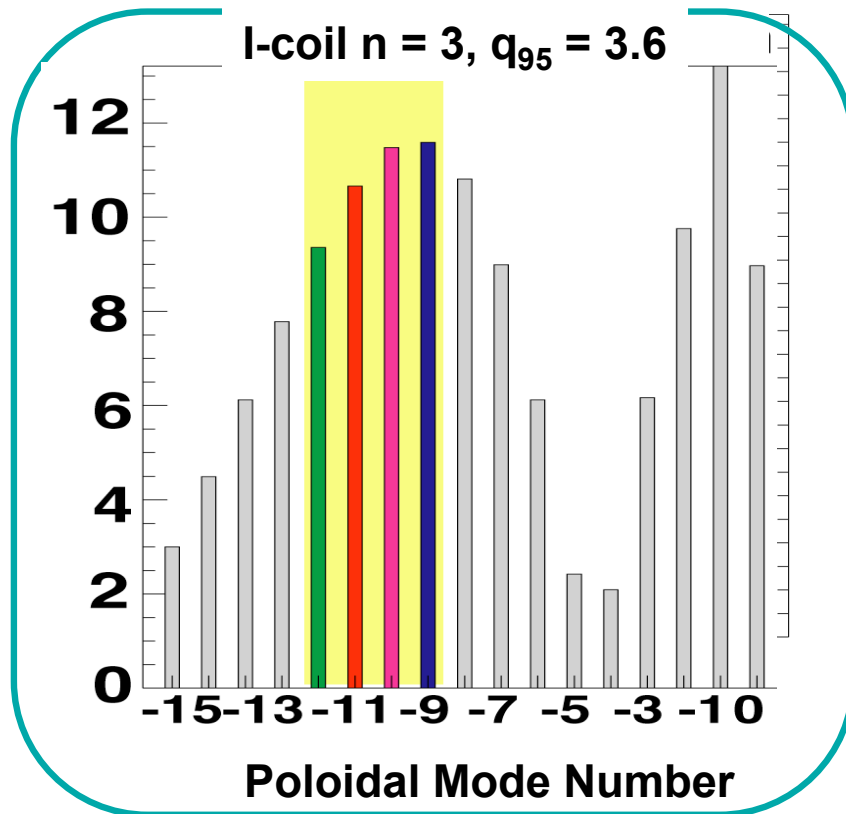
- Density profile change is largest contribution to pressure gradient reduction.

$\delta \sim 0.26$

$\delta \sim 0.53$

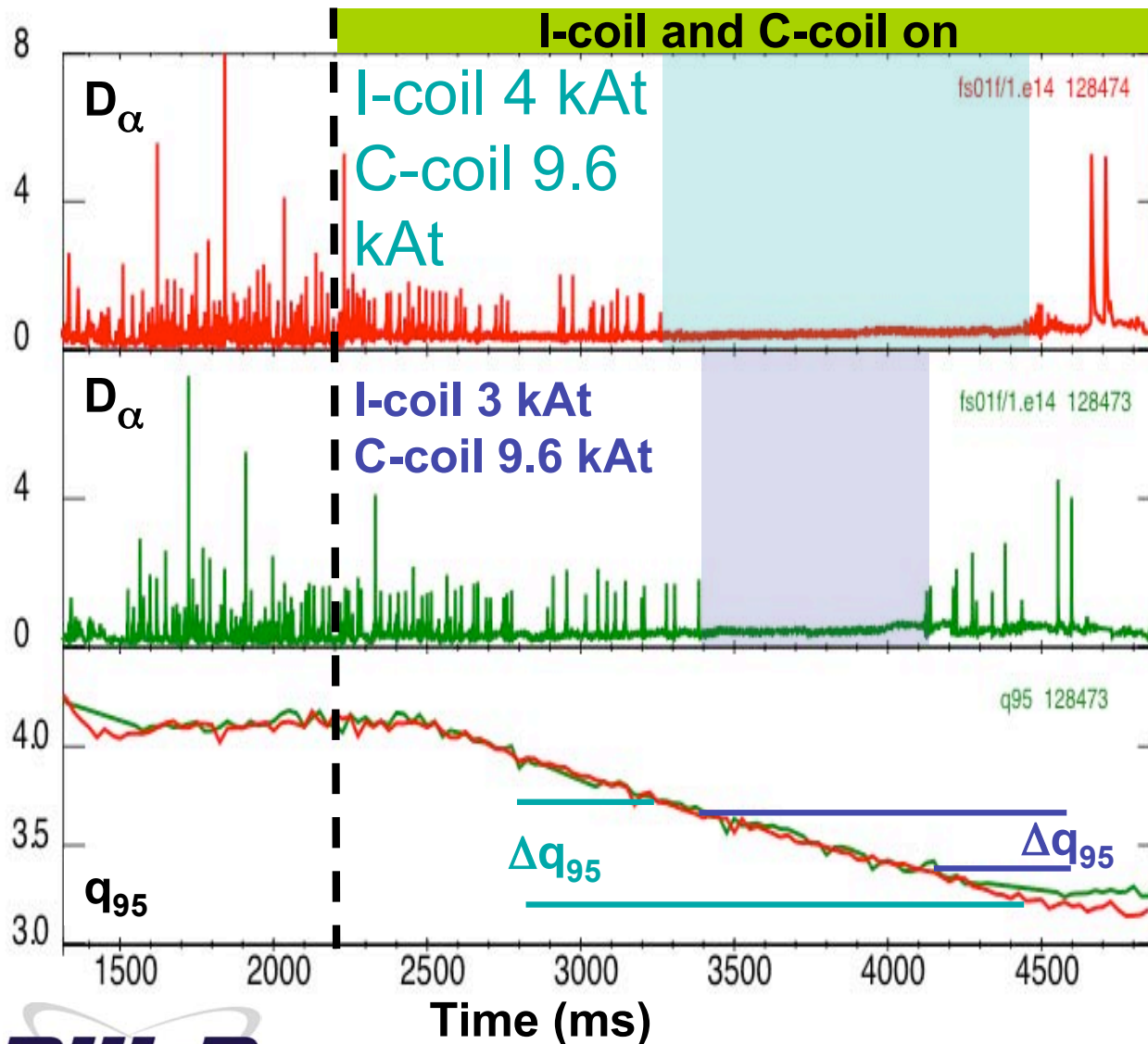


I-coil Even Parity $n=3$ Spectrum Optimum for Pitch Resonance at $q_{95} \sim 3.6$ in DIII-D



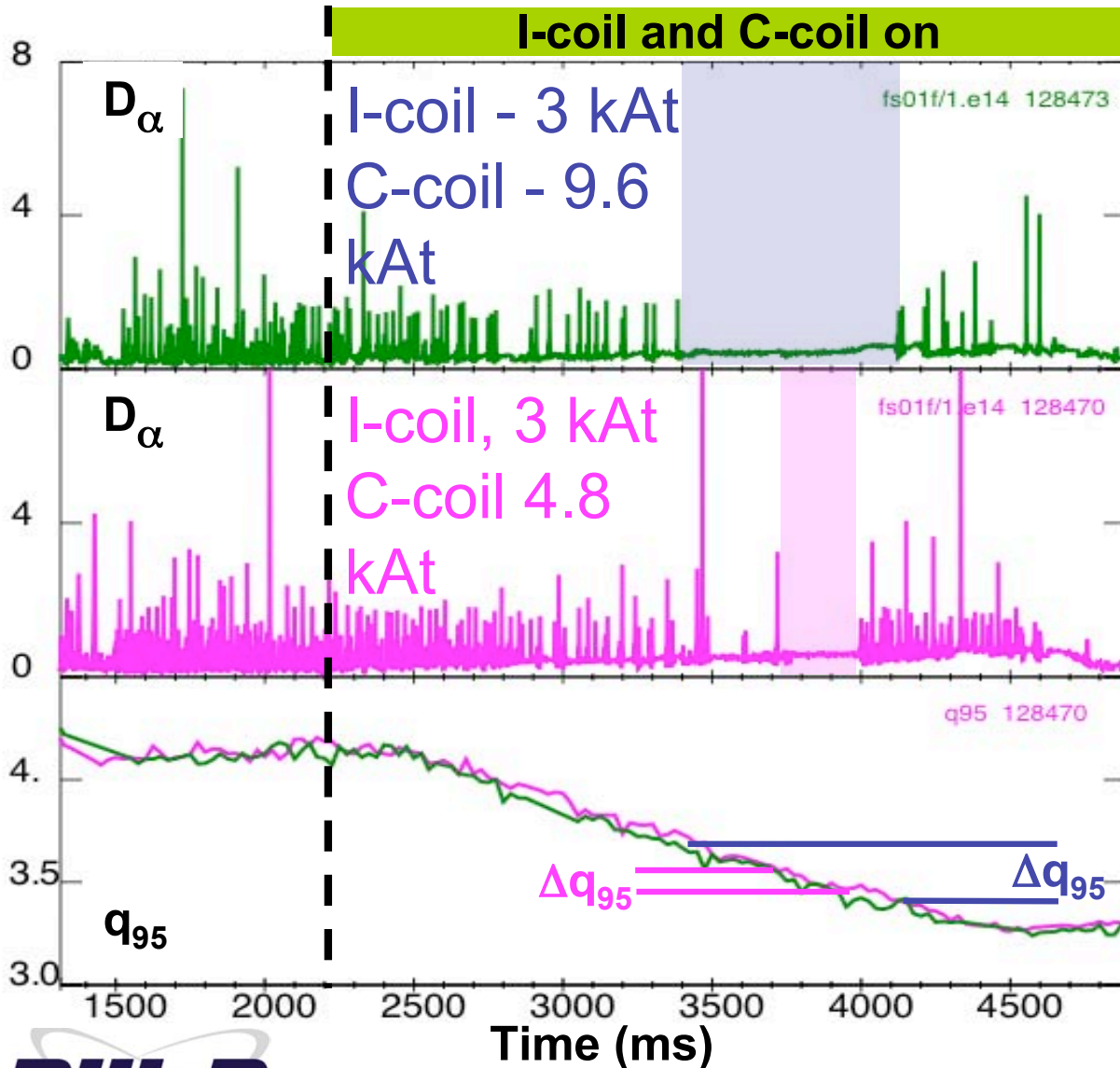
- Strength of I-coil $n=3$ RMP in pedestal depends on up/down parity of coil sets
 - Even parity (upper and lower loop δb_r same direction) gives maximum edge perturbation for $3 < q_{95} < 4$,
 - Edge perturbation $\delta b_r^{11/3}/B_T = 5 \times 10^{-4}$ at $\Psi_N = 0.95$ for 6.3 kAt

Safety Factor Resonance Window for ELM Suppression Expanded with n=3 RMP Strength



- I_p up ramps used to produce q_{95} down ramps
- Resonance window for suppression increased with I-coil current
 - At 3 kAt suppression for $\Delta q_{95} = 0.30$
 - At 4 kAt suppression for $\Delta q_{95} = 0.50$

Resonance Window in q Expanded With Additional C-coil $n=1$ Field Combined With I-coil $n=3$ RMP in Edge

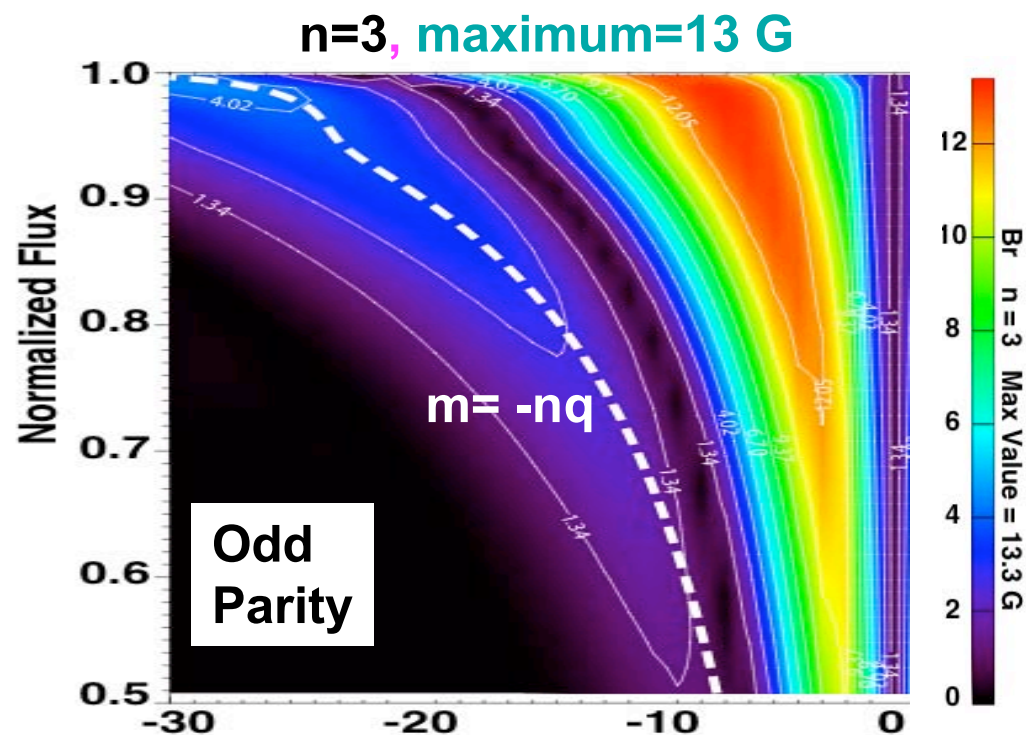
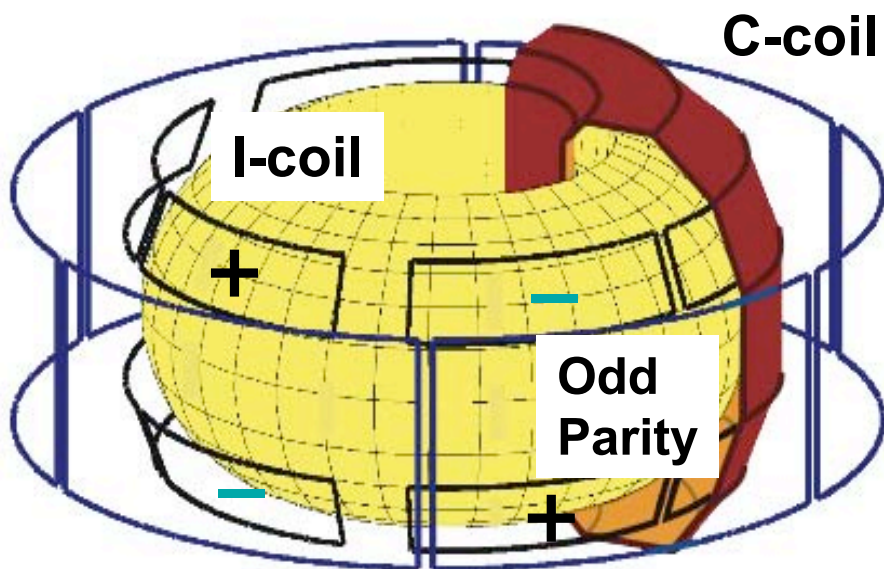


- Resonance window for suppression increased with C-coil current
 - At 4.8 kAt suppression for $\Delta q_{95} = 0.08$
 - At 9.6 kAt suppression for $\Delta q_{95} = 0.30$

- Changes seen in target particle flux splitting

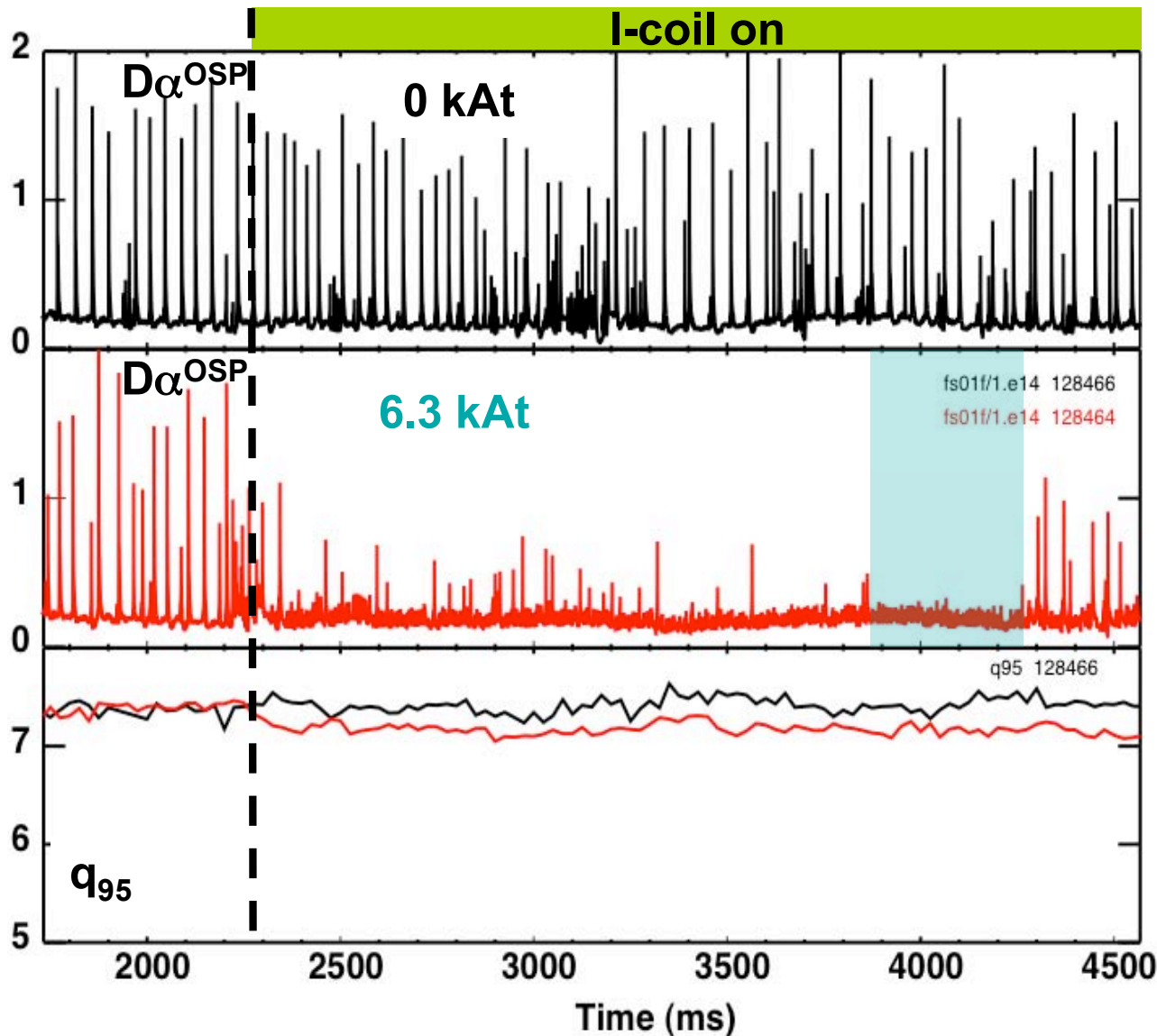
Schmitz, Joseph, Watkins
Poster session UP8 Th pm

ELM Suppression Expected for Odd Parity n=3 I-coil RMP at Pitch Resonant $q_{95} \sim 7.5$



- Edge pitch resonant lobe of spectrum aligns with q -profile for $q_{95} \sim 7.5$
- Odd parity $n=3$ produces weaker edge RMP than even parity
 - Edge perturbation $\delta b_r^{23/3}/B_T = 0.8 \times 10^{-4}$ at $\Psi_N=0.95$ for 6.3 kAt

Strong ELM Mitigation Seen for Pitch Resonant Odd Parity I-coil at High $q_{95} \sim 7.5$



- Further confirmation that suppression is a resonant effect
- Remaining ELMs (Type-I) reduced factor of 20 (D_{α}) from no RMP case

Particle balance indicates that walls must be doing most of the pumping in ELM-suppressed phase

- cryopumps exhaust particles transiently for 100–300 ms at start of I-coil pulse before ELMs are suppressed

- Increased transport & broader SOL = higher exhaust

L. Zeng UP8.00026

- Particle transport from higher frequency, smaller amplitude, more convective ELMs

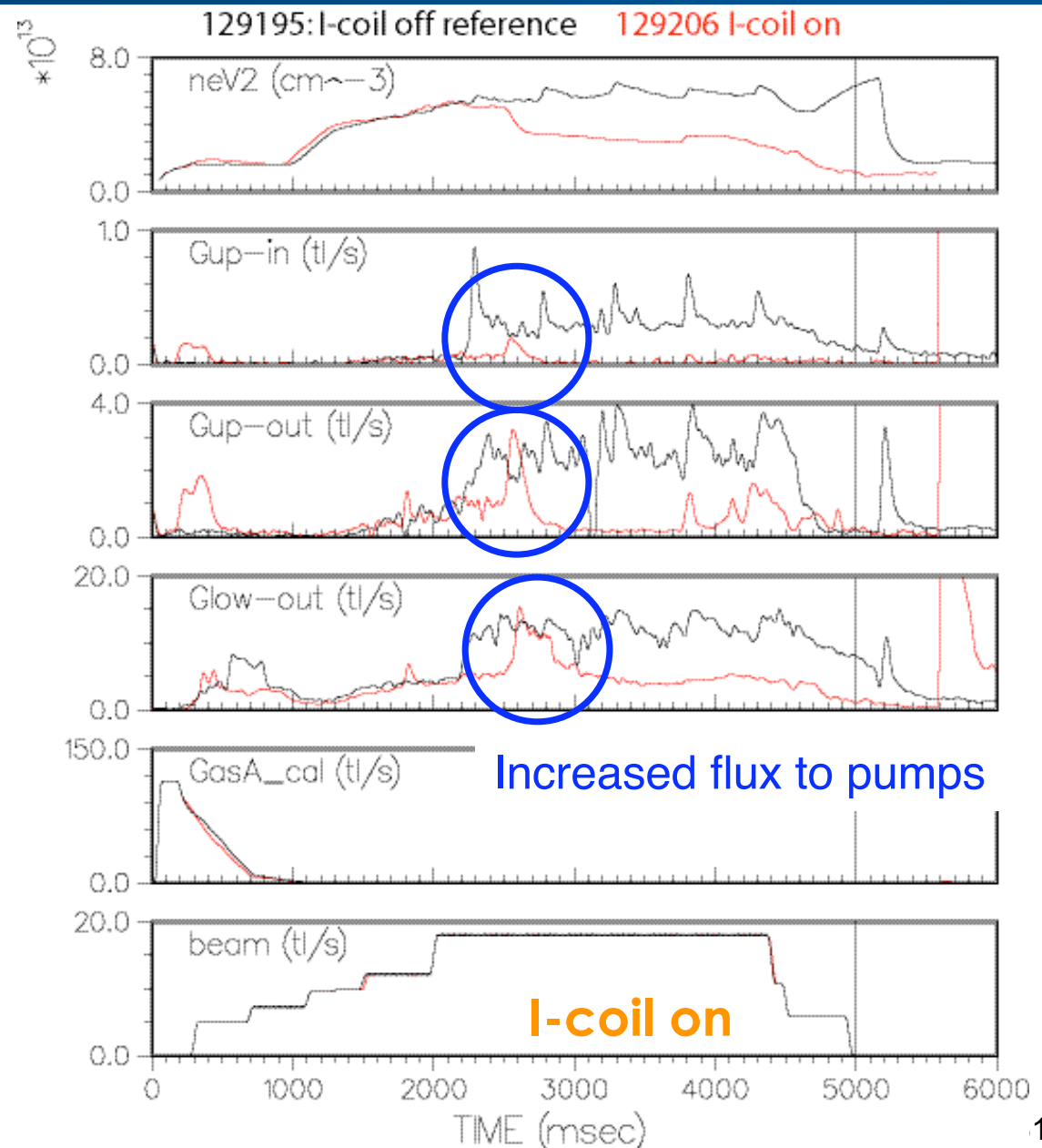
$$\Delta W_{\text{ELM}} = 5\text{--}20 \text{ kJ before RMP}$$

$$\Delta W_{\text{ELM}} = 2\text{--}5 \text{ kJ during RMP}$$

O. Schmitz UP8.00034

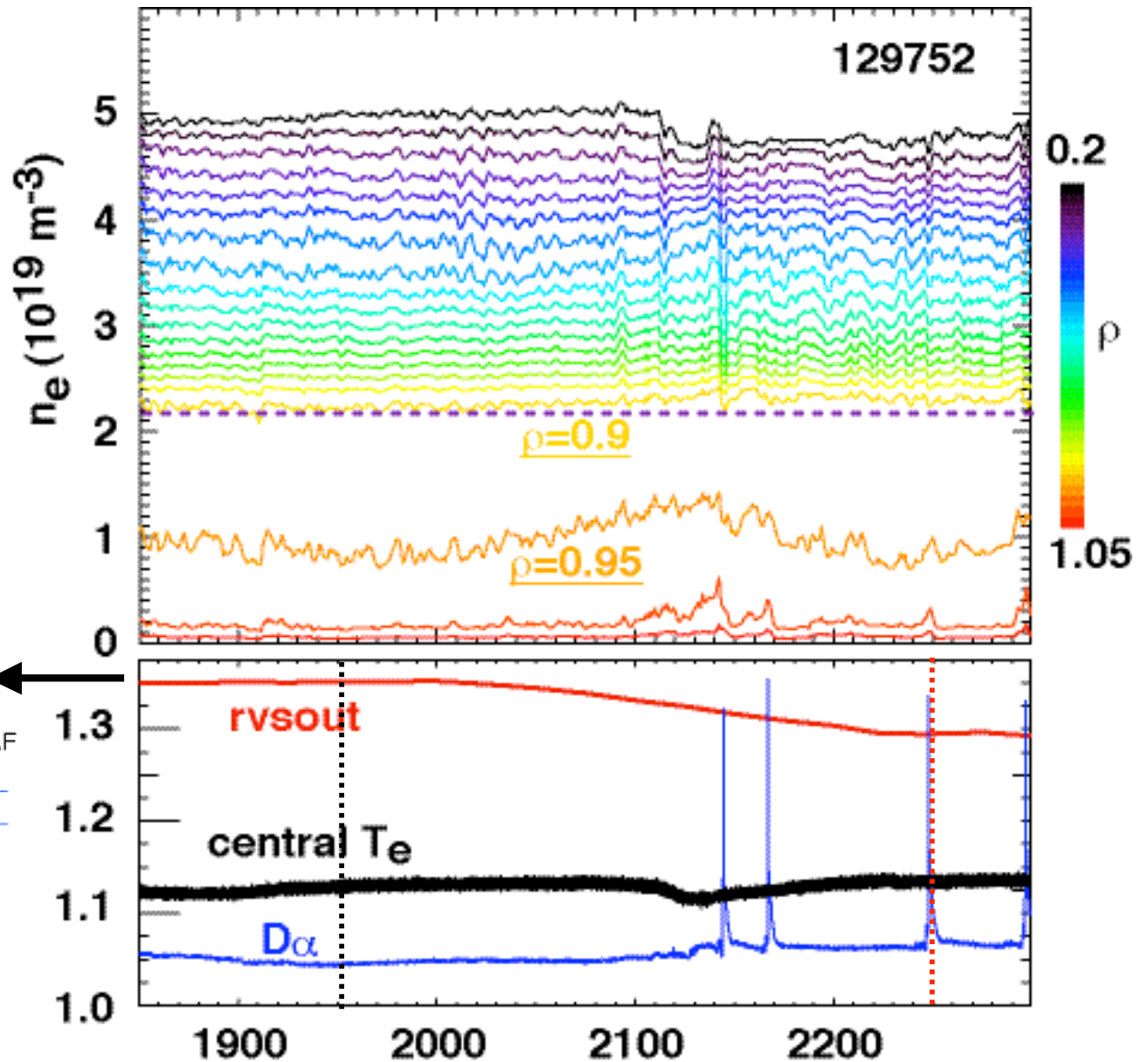
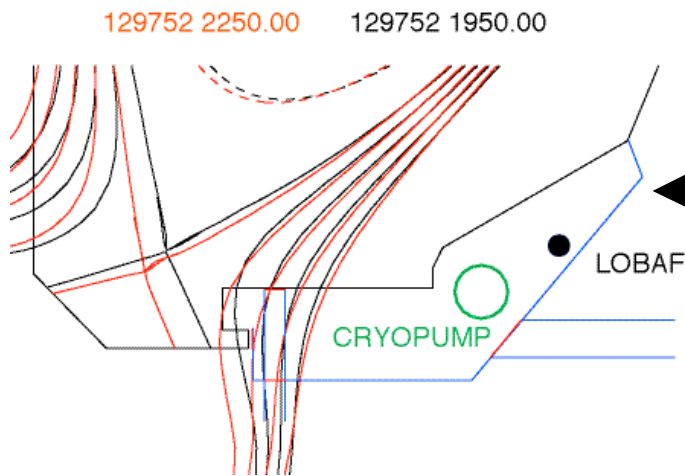
- Wall pumping (main chamber?) plays significant role once ELMs suppress

Analysis by T.W. Petrie



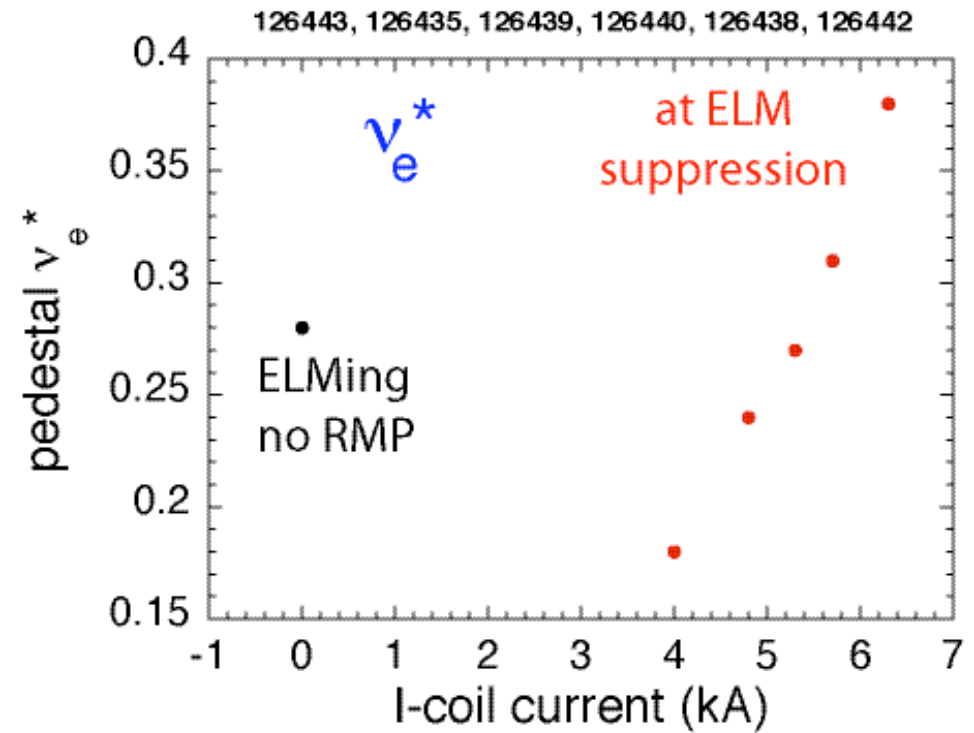
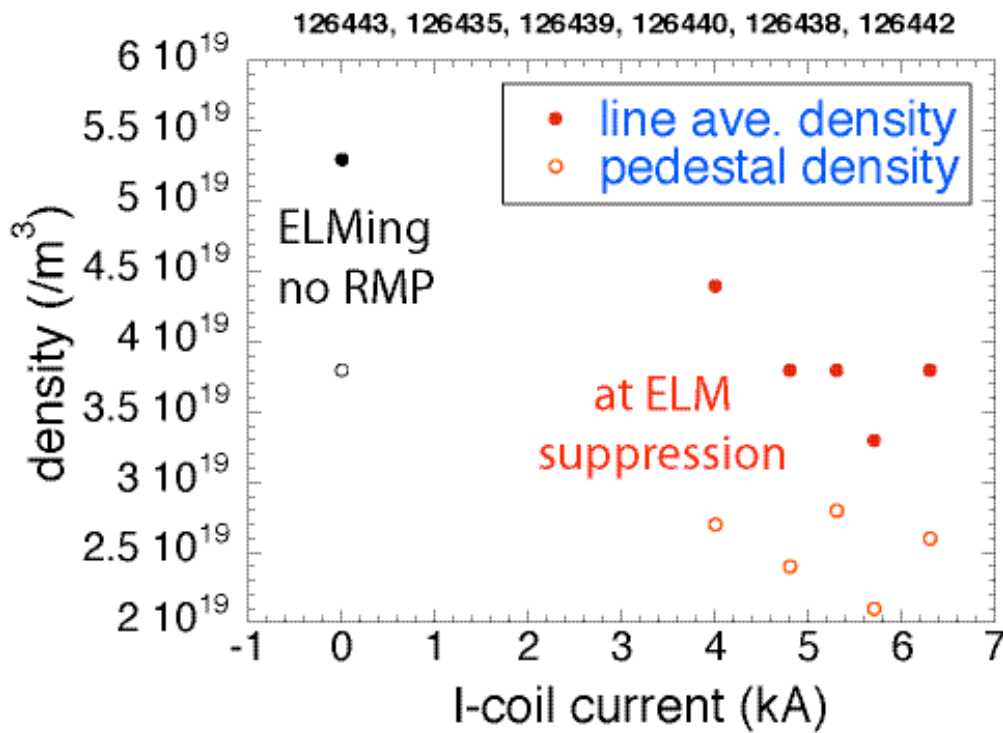
Outer strike point scan causes prompt rise in pedestal n_e and a return to ELMing H-mode

- n_e at $\rho=0.95$ ramps linearly as strike point moved away from pump



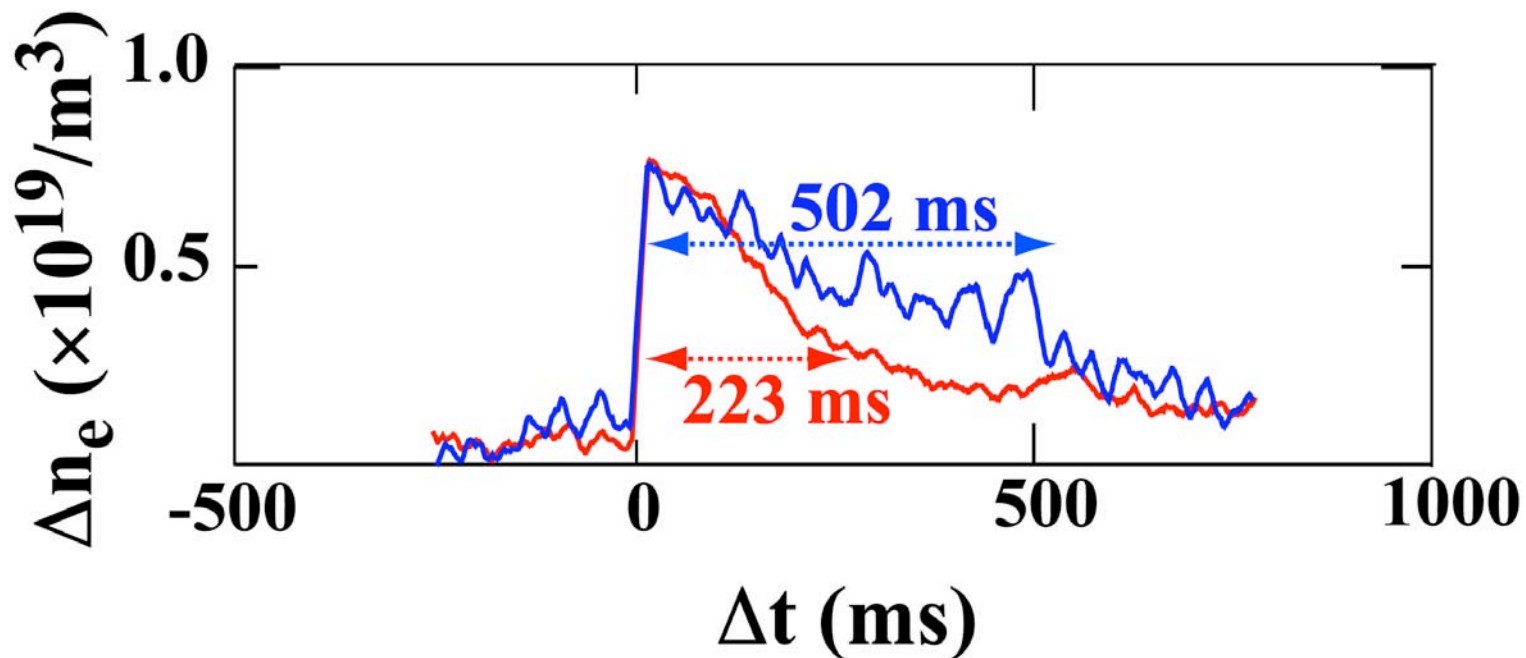
Line average density, pedestal density, and pedestal v_e^* at ELM suppression don't order the data well.

- I-coil current scan on a single day with fixed shape and power
 - line average density, pedestal density, and pedestal collisionality taken at onset of ELM suppression



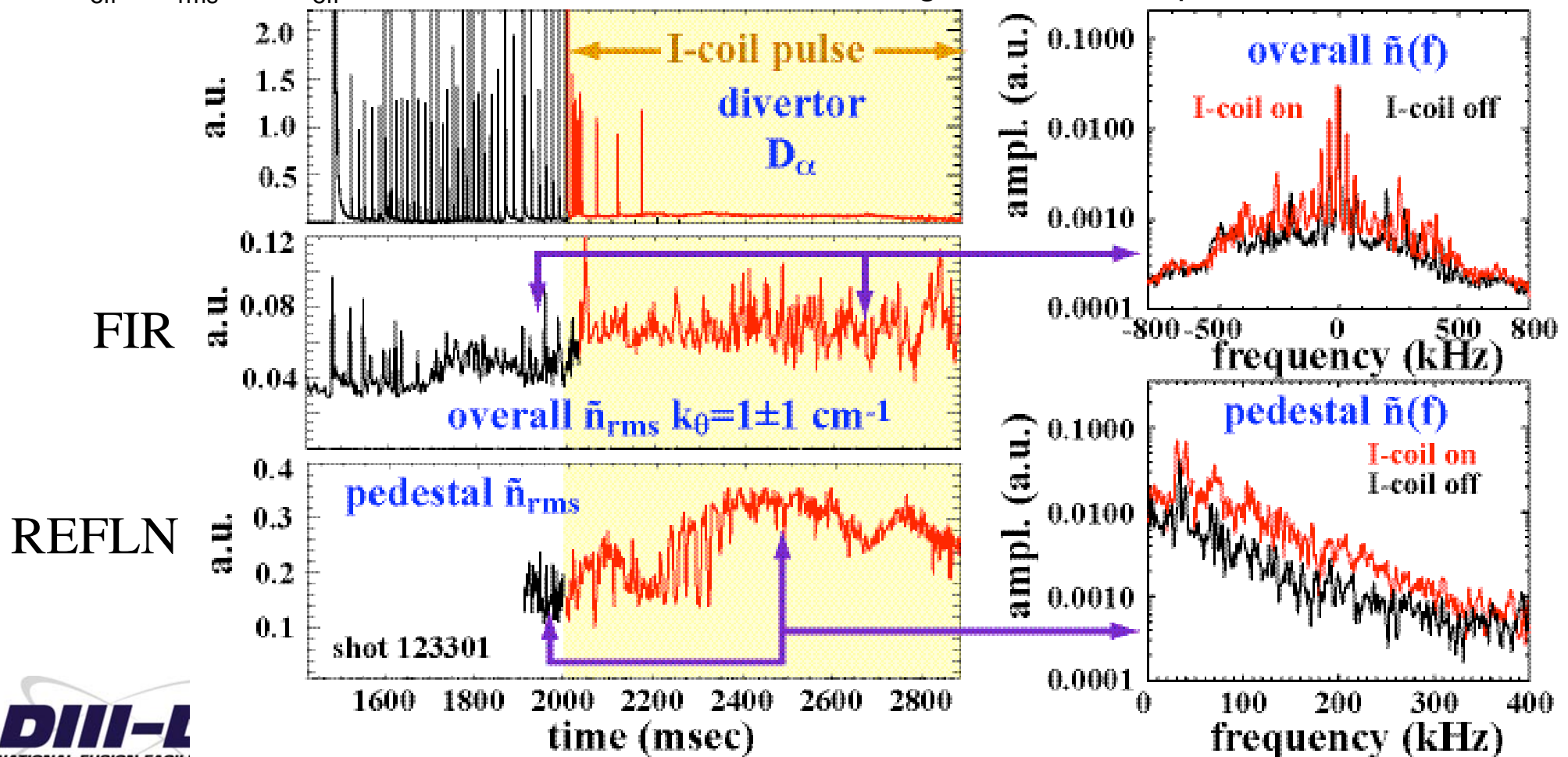
τ_p^* reduced a factor of 2 in pellet perturbation experiments with similar recycling ($\rightarrow \tau_p$ change)

- Identical pellets injected into discharges with $\nu_e^* \sim 0.2$, $\delta \sim 0.52$, and similar recycling conditions:
 - I-coil = 0 kA, ELMing H-mode
 - I-coil = 4 kA, RMP-assisted ELM-free H-mode



Increased particle transport during RMP may be due to increased fluctuation-driven transport.

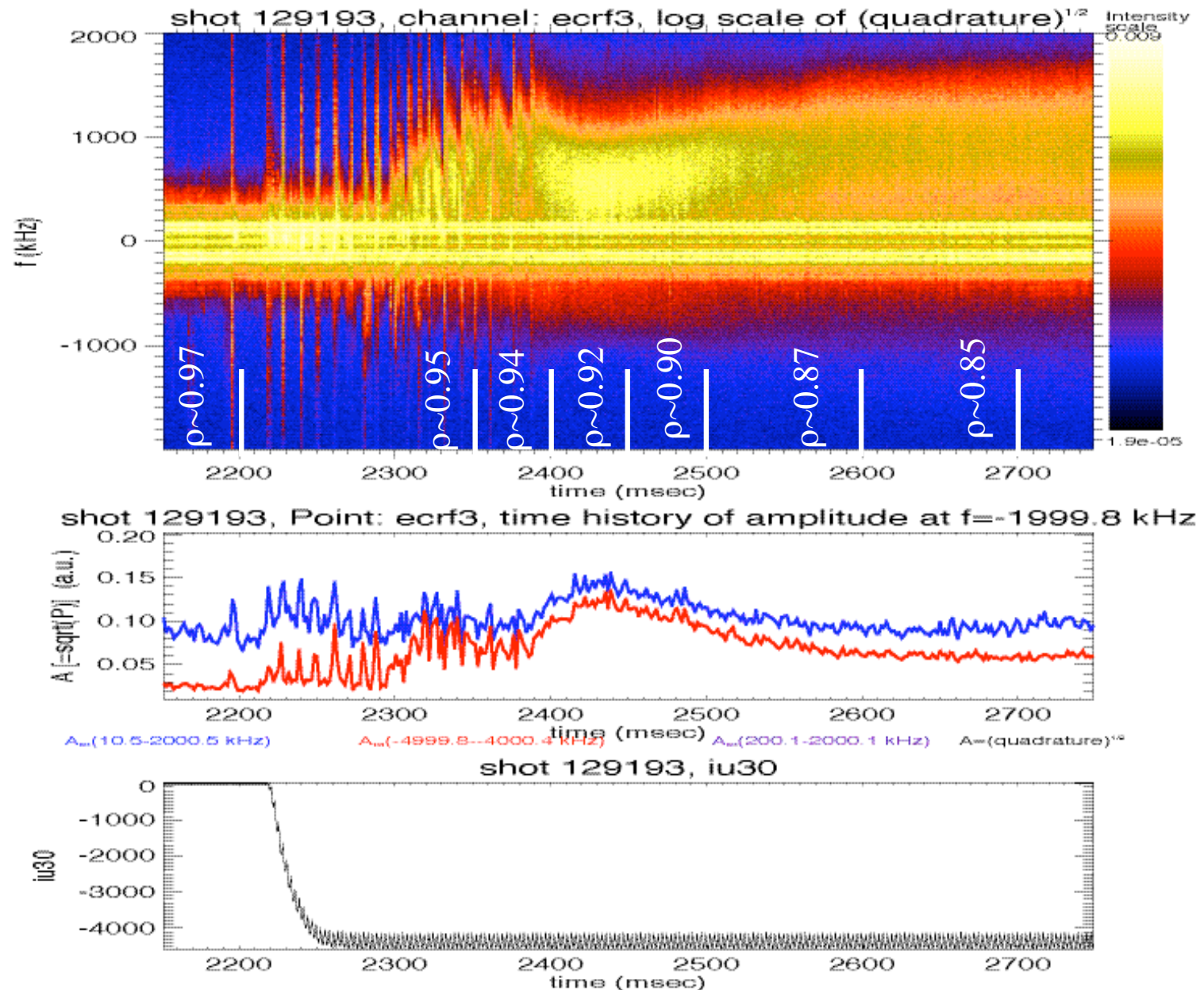
- FIR scattering: $k_\theta = 1 \text{ cm}^{-1}$ not spatially localized \rightarrow increased coherent modes and broadband turbulence \rightarrow 1.5x increase in \tilde{n}_{rms}
- reflectometry: localized to pedestal \rightarrow increased turbulence \rightarrow 2x increase in \tilde{n}_{rms}
- $D_{\text{eff}} \sim \tilde{n}_{\text{rms}}^2 \rightarrow D_{\text{eff}}$ increases 3-4x, consistent with change inferred from profiles.



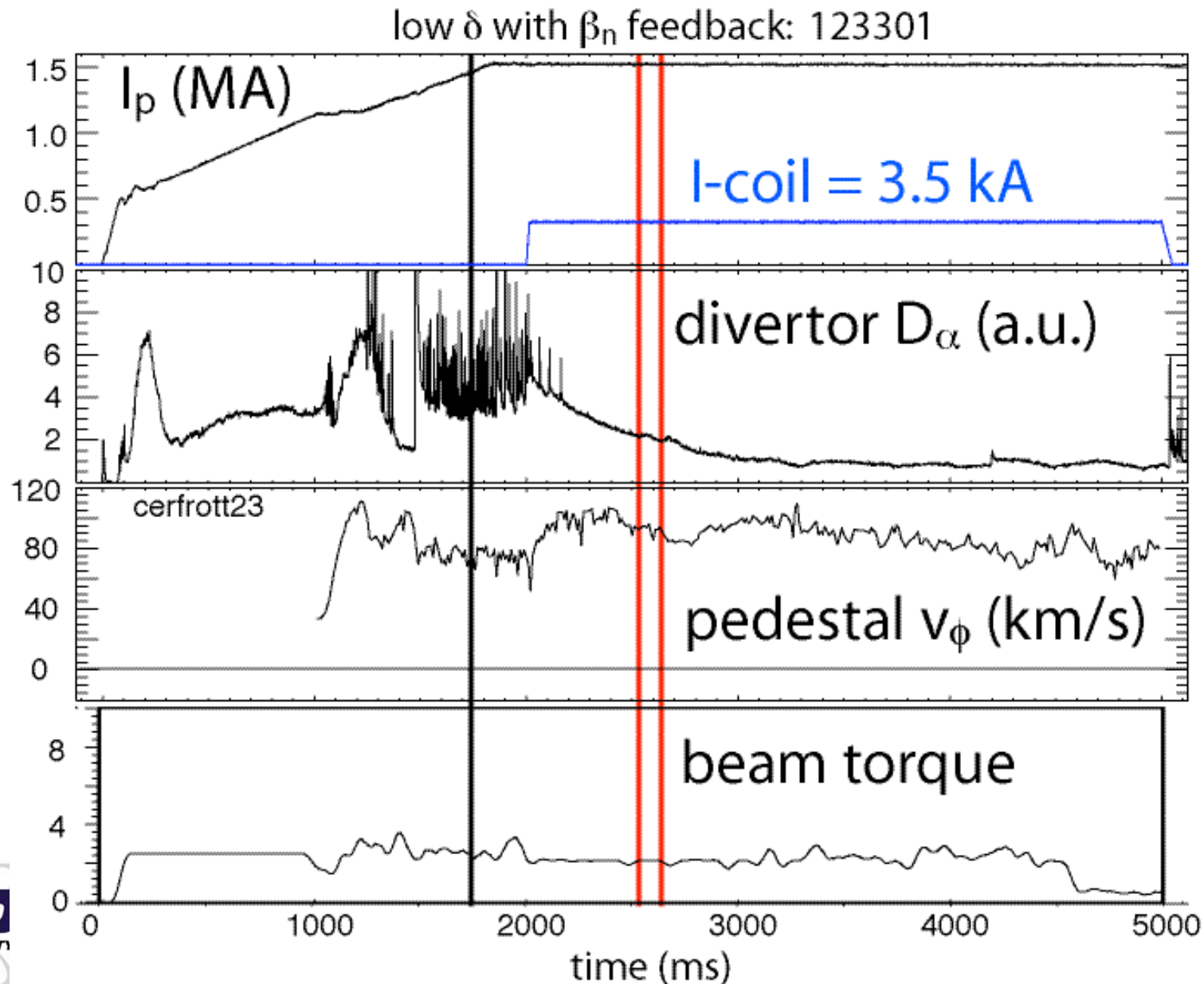
Intermediate $k_\theta \sim 4$ to 5 inv. cm also increase broadband in the pedestal at ELM suppression

- Pedestal E_r changes at 2300 ms ($\rho \sim 0.97$)
- Fluctuations increase broadband when the ELMs suppress at 2500 ms ($\rho \sim 0.90-0.94$)

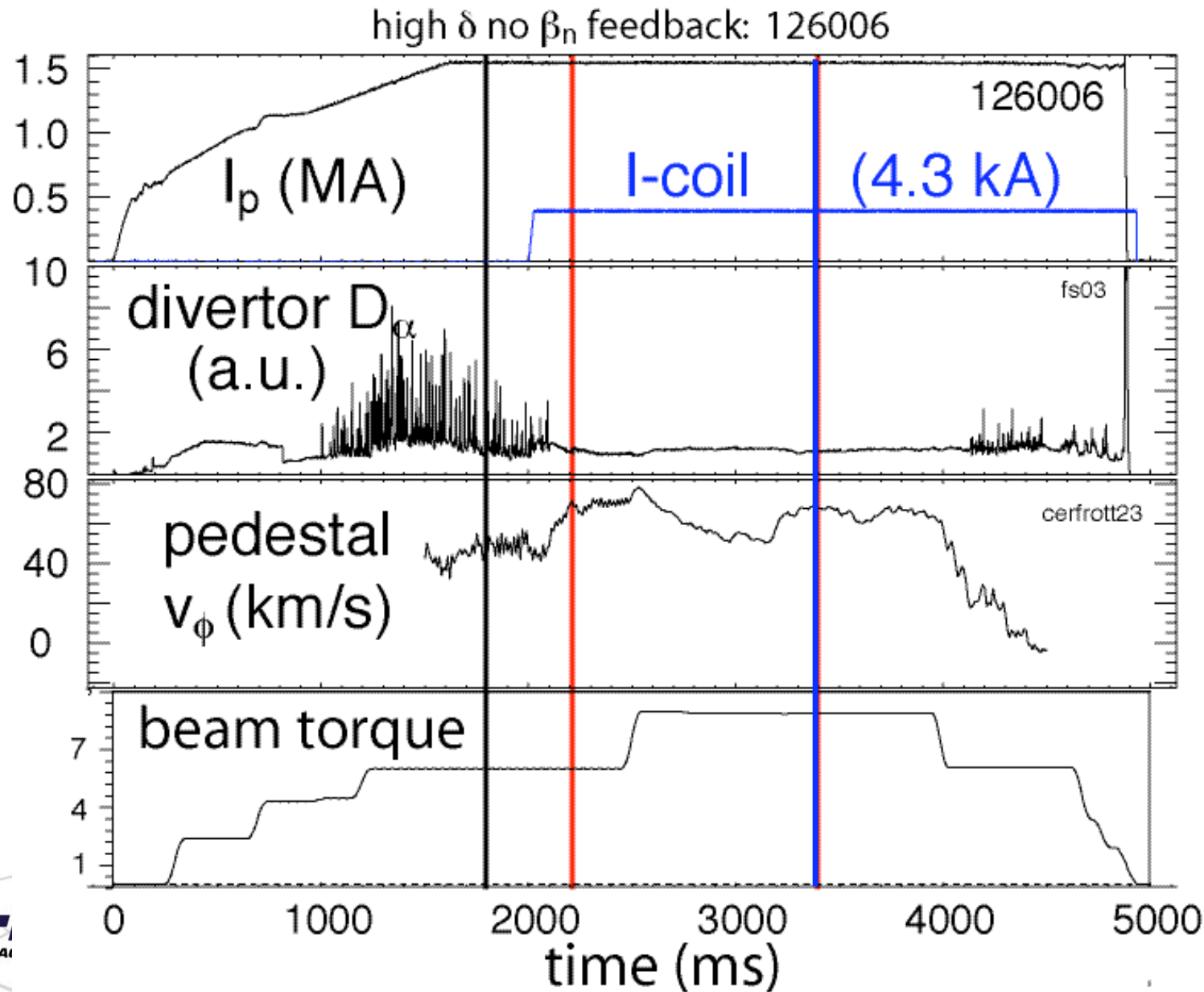
UCLA Doppler reflectometry by L Schmitz



Pedestal toroidal rotation & E_r change promptly when RMP is applied and q_{95} resonant (RMP penetrates?)



Pedestal toroidal rotation & E_r change promptly when RMP is applied and q_{95} resonant (RMP penetrates?)



Similar prompt changes in v_ϕ and E_r in high $\delta \sim 0.52$ discharges at resonant q_{95}

- E_r well shift similar to deformations in preliminary IPEC modeling.

